ALMA MATER STUDIORUM
UNIVERSITÀ DI BOLOGNA

DOTTORATO DI RICERCA IN

BIOLOGIA CELLULARE E MOLECOLARE

Ciclo 38

**Settore Concorsuale:** 05/I1 - GENETICA

**Settore Scientifico Disciplinare:** BIO/18 - GENETICA

# ADNP INTERACTIONS WITH HP1 GOVERN NEURONAL FATE

**Presentata da:** Emanuel Forciniti

**Coordinatore Dottorato**

Anna Maria Porcelli

**Supervisore**

Giovanni Perini

**Co-supervisore**

Kavitha Sarma

Esame finale anno 2026

## ABSTRACT

Chromatin regulators play essential roles in brain development by orchestrating gene expression programs that guide neural lineage specification and differentiation. Among them, Activity-dependent neuroprotective protein (ADNP) is a critical chromatin regulator whose heterozygous mutations cause ADNP syndrome, a neurodevelopmental disorder associated with autism. ADNP contributes to the regulation of chromatin accessibility and genome organization, in part through interactions with the chromatin remodeler CHD4 and heterochromatin protein HP1 to form the ChAHP complex, though additional mechanisms may also be involved. We dissected the role of these interactions in neurodifferentiation using separation-of-function mutants in mouse embryonic stem cells (mESCs) that disrupt ADNP-HP1 (ADNPΔHP1) or ADNP-CHD4 (ADNPΔCHD4) interactions. Interestingly, ADNPΔHP1, but not ADNPΔCHD4, fails to differentiate into neural progenitor cells, highlighting a critical role for HP1 in mediating ADNP function during neurodifferentiation. Genome-wide profiling revealed that HP1 and CHD4 regulate ADNP binding to distinct genomic regions, with ADNPΔHP1 showing loss at lamin-associated domains (LADs) and pericentromeric heterochromatin, leading to derepression of major satellites and neural gene targets. Additionally, ADNPΔHP1 exhibited downregulation of NANOG, a crucial pluripotency marker, and the consequent upregulation of some NANOG-target neural genes. In contrast, ADNPΔCHD4 alters ADNP binding at promoters and CTCF-enriched sites without impairing neurodifferentiation, indicating distinct functional contributions of these interactions. Our findings highlight distinct contributions of ADNP interactions with HP1 and CHD4 in chromatin regulation and neural gene expression and point to a broader role of ADNP–HP1 interactions in orchestrating early neurodevelopmental programs, including those controlled by pluripotency factors such as NANOG.

# INDEX

## INTRODUCTION

Chromatin organization lies at the heart of eukaryotic genome regulation, shaping how genetic information is accessed, expressed, and maintained. The eukaryotic genome is not a linear entity but a highly ordered three-dimensional structure that integrates multiple layers of organization and regulation. At its foundation, DNA is wrapped around histone proteins to form nucleosomes—the fundamental repeating units of chromatin. Nucleosomes are organized into fibers that can assume either open or compact structures, known respectively as euchromatin and heterochromatin, which correspond to the level of transcriptional activity (Grewal and Moazed, 2003; Kornberg and Lorch, 1999). At higher levels, chromatin is partitioned into topologically associating domains (TADs), which serve as self-interacting regions that coordinate enhancer-promoter communication and constrain regulatory interactions (Dixon et al., 2012). TADs are further organized into A and B compartments, broadly corresponding to transcriptionally active and inactive chromatin, and entire chromosomes occupy distinct territories within the nucleus, preserving the spatial logic of the genome (Lieberman-Aiden et al., 2009).

Far from representing a static scaffold, chromatin constitutes a dynamic and responsive framework that governs genome function, stability, and cellular identity. Its organization is actively shaped by a network of regulatory factors, including histone-modifying enzymes, ATP-dependent chromatin remodelers, DNA methylation machinery, and architectural proteins. Together, these elements orchestrate the establishment, maintenance, and remodeling of chromatin states that underlie developmental programs and cellular responses to environmental cues. Understanding the principles and molecular mechanisms that govern chromatin architecture is therefore fundamental to unraveling the epigenetic logic of gene regulation in health and disease.

The proper execution of developmental programs requires precise regulation of gene expression, which is orchestrated not only by transcription factors but also by chromatin and epigenetic regulators. Chromatin-modifying enzymes and complexes—including histone methyltransferases, acetyltransferases, ATP-dependent remodelers, and heterochromatin-binding proteins—control the accessibility of genomic regions, thereby guiding cell fate decisions (Chen and Dent, 2014). By establishing active or repressive chromatin states, these regulators coordinate the timing and sequence of lineage specification, maintain pluripotency in embryonic stem cells (ESCs), and ensure faithful execution of developmental programs (Atkinson and Armstrong, 2008). Dysregulation of chromatin architecture or

epigenetic modifications can result in aberrant gene expression, premature or delayed differentiation, and developmental disorders, highlighting the central role of chromatin and epigenetic regulators in organismal development (Dominguez et al., 2024; Rezazadeh et al., 2025).

## CHROMATIN BASIS OF NEURAL DEVELOPMENT

Neural development is an intricate and tightly regulated processes that leads to the definition of the central and peripheral nervous systems starting from a population of pluripotent ESCs This transformation depends on the integration of signaling pathways, transcriptional regulators, chromatin dynamics, and genome architecture to ensure temporal precision and spatial specificity. Neural development provides a unique paradigm in which cell fate, genome regulation, and three-dimensional nuclear organization converge to generate functional complexity. Unravelling the mechanisms that regulate these processes is crucial for the potential therapeutical development in the fields of regenerative medicine, stem cell therapy, and the treatment of neurodevelopmental disorders.

### From Pluripotency to Neural Induction

ESCs, derived from the inner cell mass of the mammalian blastocyst, are characterized by their ability to self-renew indefinitely while retaining the potential to differentiate into all somatic lineages. A major transition in early embryogenesis is the specification of the ectoderm into neural versus non-neural fates (Muñoz-Sanjuán and Brivanlou, 2002; Wilson and Edlund, 2001). At the molecular level, the first step is the exit from pluripotency stage. This change is orchestrated by stage-specific transcription factors that sequentially activate and repress gene expression programs. Pluripotency factors such as Pou5f1 (Oct4), Sox2, Klf4 and Nanog maintain the ESC state (Takahashi and Yamanaka, 2006; Wang et al., 2008), but upon neural induction, Sox2 is repurposed in combination with Sox1, Pax6, and Hes family members to specify neural progenitor identity, along with a strong repression of Nanog and Pou5f1 (Stevanovic et al., 2021; Zhang et al., 2019). The onset of proneural factors, including Neurog2, Neurod1, Ascl1, and Olig2 drives later steps of neuronal differentiation (Bertrand et al., 2002). Collectively, these signals bias ectodermal cells toward a neural fate, establishing the neuroectoderm and giving rise to the earliest morphological precursor of the nervous system.

Transcriptional regulation is not a linear process but instead relies on feedback loops, cross-repression, and integration with morphogen signalling pathways. For example, Notch signalling maintains progenitor pools by inducing Hes genes, which repress proneural TFs, while Shh and Wnt signals act in spatially restricted domains to bias differentiation toward ventral or dorsal neuronal subtypes (Gozlan and Sprinzak, 2023; Jessell, 2000). Thus, transcription factors act as molecular interpreters of extracellular cues, linking positional information to cell-intrinsic programs.

**Chromatin Dynamics and Epigenetic Control**

Neural development is accompanied by profound remodelling of the epigenome. Histone modifications mark the transition from pluripotency to lineage commitment:

- Repressive marks such as H3K27me3 and H3K9me3 silence pluripotency genes and restrict alternative lineage programs.
- Active marks such as H3K4me3 and H3K27ac accumulate at neural enhancers, enabling robust expression of fate determinants.

A hallmark of lineage commitment is the resolution of bivalent chromatin domains, in which activating and repressive marks coexist at key developmental genes in ESCs (Jessell, 2000; Park et al., 2022). During neural differentiation, these domains resolve into either active or repressed states, thereby locking in cell fate.

DNA methylation further contributes to lineage restriction, both by silencing non-neural programs and stabilizing neural identity. The dynamics of DNA methylation and hydroxymethylation (via TET enzymes) are especially critical in regulating enhancers during neuronal maturation (MacArthur and Dawlaty, 2021; Wu et al., 2011).

The three-dimensional genome architecture also plays a fundamental role in neural development. Topologically associating domains (TADs) and long-range enhancer–promoter loops allow precise regulation of developmental genes such as Sox2, Olig2, and Dlx. Chromatin architectural proteins, including CTCF and cohesin, dynamically reorganize during neural differentiation, enabling the activation of neural enhancers while insulating non-neural regions (Bonev et al., 2017; Fudenberg et al., 2016).

Spatial compartmentalization within the nucleus also contributes to fate transitions. Genes required for neural identity are relocated to transcriptionally active compartments, while

pluripotency or alternative lineage genes are localized into repressive genomic regions such as the lamina-associated domains (LADs). LADs are large genomic regions that physically contact the nuclear lamina, a filamentous protein network underlying the inner nuclear membrane that provides structural support to the nucleus and interfaces with chromatin. LADs are typically enriched in transcriptionally silent chromatin, characterized by repressive histone modifications such as H3K9me2/3 (Briand and Collas, 2020; Martin et al., 2025).

LADs play a key role in shaping higher-order genome organization and contribute to the maintenance of cell-type–specific transcriptional programs. During differentiation, extensive LADs reorganization occurs, with developmental genes relocating, reflecting the dynamic regulation of gene expression. Dysregulation of LADs organization has been implicated in laminopathies, aging, and neurodevelopmental disorders, underscoring their importance for cellular identity and genome stability (Martin et al., 2025; van Steensel and Belmont, 2017).

Despite recent advances, the mechanisms that determine LAD positioning and dynamics remain incompletely understood. The interplay between lamina proteins, chromatin regulators, and transcription factors in establishing and maintaining LADs is an area of active investigation, with significant implications for understanding genome function in development and disease.

**Heterochromatin and Transposable Element Control**

Neural development also requires the silencing of transposable elements (TEs) and the stabilization of heterochromatin (Ilık İ et al., 2025). Retrotransposons, which make up nearly half of mammalian genomes, pose a potential threat to genome stability through mobilization and insertional mutagenesis. In ESCs and neural progenitors, a network of heterochromatin regulators, including HP1 proteins, SETDB1, and KAP1, ensures TE repression through H3K9me3-mediated silencing (Hutnick et al., 2010; Karimi et al., 2011).

Interestingly, TEs are not solely detrimental. Many neural enhancers are derived from transposable element sequences, which have been co-opted during evolution to provide regulatory diversity. For example, TE-derived enhancers contribute to the expression of genes involved in cortical development and neuronal identity (Chuong et al., 2017; Diehl et al., 2020; Notwell et al., 2015). Thus, the regulation of TEs represents a balance between genome defence and regulatory innovation in neural development.

**Perspectives on neural differentiation**

Neural development exemplifies the convergence of cellular morphogenesis with molecular and genomic regulation. From transcription factors that interpret positional cues, to chromatin landscapes that stabilize lineage decisions, to nuclear architecture that shapes enhancer–promoter communication, multiple layers of regulation act in concert to generate the nervous system.

Disruptions at any of these levels can lead to profound neurodevelopmental disorders. Advances in single-cell multi-omics and stem-cell–derived neural models now provide unprecedented opportunities to dissect these processes with high resolution (Kim et al., 2024; Qian et al., 2019; Velmeshev et al., 2019). A comprehensive understanding of how gene regulation, genome architecture, heterochromatin, and transposable elements intersect to shape neural development is not only a fundamental question in biology but also a prerequisite for therapeutic strategies in regenerative medicine and neurological disease. Among key regulators, the Activity Dependent Neuroprotective Protein (ADNP) has emerged as a critical modulator of chromatin remodeling and transcriptional control during neurodevelopment, with mutations in ADNP linked to autism spectrum disorder and other neurodevelopmental conditions (Clémot-Dupont et al., 2025; D'Incal et al., 2023).

Because of its complexity, neural development is highly vulnerable to perturbations. Genetic mutations or signalling imbalances can result in developmental disorders with lifelong consequences. At the same time, the ability to recapitulate aspects of neural development using ESCs or induced pluripotent stem cells (iPSCs) has revolutionized neuroscience research, providing platforms to model disease, test therapeutics, and explore regenerative strategies (Pașca et al., 2019; Shi et al., 2012). ADNP plays a pivotal role in neural differentiation from pluripotent stem cells, modulating chromatin accessibility and Wnt/β-catenin signaling to guide lineage specification and cortical development (Bieluszewska et al., 2025; Sun et al., 2020). A comprehensive understanding of how pluripotent cells generate the nervous system is therefore critical not only for developmental biology but also for translational medicine.

## ADNP

ADNP is a chromatin regulator that is essential for brain development. It is characterized by nine zinc-fingers and a homeodomain responsible for chromatin association (Figure 1).

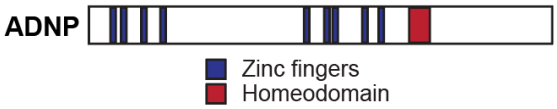


**Figure 1 ADNP protein structure**

ADNP heterozygous mutations cause ADNP syndrome, a neurodevelopmental disorder which based on its frequency in the population was proposed as one of the more frequent single gene causes of autism (Helsmoortel et al., 2014). Clinically, ADNP syndrome presents with a heterogeneous phenotype, though several features are highly penetrant. These include global developmental delay, moderate to severe intellectual disability, speech and motor impairment, hypotonia, and autism spectrum disorders (Helsmoortel et al., 2014). At the molecular level, ADNP mutations are typically heterozygous truncating variants that insert a premature stop codon, usually at C-terminal region of the protein. To this day, the molecular mechanism leading to the onset and progression of ADNP syndrome remain poorly understood. ADNP knock out in mouse models results in early embryonic lethality due to a defect in neural tube closure (Pescosolido et al., 2014). In contrast, heterozygous *Adnp* knockout mice (*Adnp*^+/−) are viable and have been used extensively to model the human condition. These mice display a range of phenotypes that partially recapitulate clinical features observed in individuals with ADNP syndrome, including impaired motor coordination, cognitive deficits, anxiety-like behaviors, and social interaction abnormalities (Gozes, 2020). ADNP deletion or mutation in cell culture models compromises the potential for embryonic stem cells to differentiate into neural progenitors (Clémot-Dupont et al., 2025; Ostapcuk et al., 2018; Sun et al., 2020). In vitro models have provided important mechanistic insights into the cellular consequences of ADNP loss or mutation. Knockout of *Adnp* in mouse ESCs impairs neural differentiation by destabilizing β-catenin and suppressing Wnt/β-catenin signaling, a pathway essential for neuroectoderm specification. Transcriptomic analyses indicate that ADNP deficiency results in aberrant gene expression and lineage priming, suggesting downstream effects on chromatin-regulated programs. In neuronal cell lines and patient-derived iPSCs carrying pathogenic ADNP mutations, researchers have observed altered subcellular localization of the protein, reduced neuronal

survival, and impaired neurite outgrowth (Bieluszewska et al., 2025; D'Incal et al., 2023; Gozes, 2020; Sun et al., 2020). Together, these studies highlight the central role for ADNP in neurodevelopment and brain function.

**The ChAHP complex**

Recent studies show that ADNP interacts with the chromodomain 4 (CHD4) chromatin remodeler and the heterochromatin protein 1 (HP1) to form the ChAHP complex (Ostapcuk et al., 2018). CHD4, an ATP-dependent chromatin remodeler of the CHD family, influences gene expression and DNA accessibility through nucleosome repositioning and interactions with multiple protein complexes. Beyond its well-known role in the NuRD complex, CHD4 also functions independently in processes such as DNA damage repair, replication, and developmental gene regulation (Farnung et al., 2020; Hoffmann and Spengler, 2019; Smeenk et al., 2010). HP1 is a conserved reader of histone H3 lysine 9 trimethylation (H3K9me3), playing key roles in heterochromatin formation, transcriptional repression, and genome stability (Ostapcuk et al., 2018). HP1 is expressed in three isoforms (HP1α, HP1β, and HP1γ), among which HP1γ has been identified as the predominant isoform interacting in the ChAHP complex. HP1γ interacts with ADNP through recognition of a canonical PxVxL motif located within the C-terminal region of ADNP (D'Incal et al., 2023; Jensen and Lorincz, 2018; Mandel et al., 2007). In contrast, the molecular basis of CHD4 recruitment to ADNP is less well defined; however, experimental evidence indicates that this interaction is mediated by the first 228 amino acids of ADNP (Ostapcuk et al., 2018). Functionally, the ChAHP complex plays a critical role in maintaining pluripotency and regulating lineage specification during early embryogenesis. Genetic ablation of ChAHP components in mESCs results in spontaneous differentiation, characterized by premature activation of lineage-specific transcriptional programs and a diminished capacity to adopt neuronal fates. Mechanistically, the repressive activity of the ChAHP complex is distinct from canonical HP1-mediated silencing. In classical heterochromatin formation, HP1 proteins cooperate with trimethylated H3 lysine 9 (H3K9me3) to establish broad, transcriptionally inert chromatin domains (Lachner et al., 2001; Maison and Almouzni, 2004). By contrast, ChAHP-dependent repression generates localized chromatin inaccessibility within otherwise euchromatic regions, thereby limiting transcription factor occupancy and preventing aberrant gene activation, whereby chromatin compaction is induced directly at ChAHP-bound loci, independent of H3K9me3 enrichment (Ahel et al., 2024; Ostapcuk et al., 2018). Recent

evidence suggests that the ChAHP complex has a role in regulation of genome organization. ChAHP antagonizes the binding of CCCTC-binding factor (CTCF), a key insulator protein responsible for establishing chromatin loops and demarcating topologically associating domains (TADs) by functioning as a barrier to loop extrusion by the cohesin complex. ADNP and CTCF share overlapping DNA recognition motifs, and competitive binding by ChAHP components at these loci impedes CTCF occupancy, thereby influencing higher-order chromatin architecture and constraining distal enhancer-promoter interactions (Kaaij et al., 2019).

**ADNP in pericentromeric heterochromatin organization**

Euchromatin refers to the less condensed, transcriptionally active regions of the genome, while heterochromatin is densely packed and generally transcriptionally silent, forming large domains particularly enriched at pericentromeric and telomeric regions that contribute to nuclear organization and genome stability. Pericentromeres are heterochromatic domains flanking the centromere that play essential roles in chromosome stability, nuclear organization, and faithful segregation during cell division (Guenatri et al., 2004). In the mouse genome, pericentromeres are largely formed by major satellite DNA (MSR), consisting of tandem repeats of a 234 bp unit spanning several megabases. Major satellites are characterized by their dense DNA methylation, enrichment in H3K9me3 and H4K20me3, and strong association with HP1 proteins (Bulut-Karslioglu et al., 2012; Maison and Almouzni, 2004). ADNP is recruited at pericentromeres by HP1 through H3K9me3 recognition, in order to repress major satellite transcription.

Despite their repressive nature, major satellite sequences are not transcriptionally inert. Under certain physiological conditions, such as early embryonic development, cellular stress, or during mitosis, they can be transcribed into noncoding RNAs. These transcripts have been implicated in the establishment and maintenance of heterochromatin, centromere function, and chromosomal architecture (Khalil and Driscoll, 2010). Within the nucleus, pericentromeric repeats cluster into chromocenters, which appear as DAPI-bright foci where heterochromatin from multiple chromosomes coalesces (Guenatri et al., 2004). These structures are not only a hallmark of nuclear organization but also serve as hubs that stabilize interactions among pericentromeric regions and contribute to overall genome compartmentalization. Defects in MSR thigh regulation have dramatic impact on cellular homeostasis. Studies have shown that overexpression of MSR RNAs induces chromosomal

instability, characterized by micronuclei formation, anaphase bridges, and activation of the DNA damage response (Fonseca-Carvalho et al., 2024). This heightened instability can sensitize cells to genotoxic agents, as observed in certain mouse cancer cell lines (Tamaki et al., 2022). Moreover, the overaccumulation of MSR transcripts can disrupt the phase separation properties of heterochromatin, leading to a more compact and static chromatin state that impairs proper gene silencing and chromatin safeguard in mouse embryonic fibroblast cells (Larson et al., 2017).

ADNP was also discovered to be enriched at pericentromeric heterochromatin (Mosch et al., 2011). To date, the distinct contributions of the ADNP–HP1 and ADNP–CHD4 interactions to the molecular functions of ADNP remain unknown, particularly regarding their role in neurodifferentiation.

**ADNP in retrotransposons regulation**

Retrotransposons, along with DNA transposons, are transposable elements (TE), mobile genetic sequences that constitute a substantial portion of the mouse genome, accounting for nearly 40–50% of genomic DNA, and they represent a risk to genome integrity because of their capacity to replicate and integrate at novel genomic sites (Bhat et al., 2022; Du et al., 2024). These elements are highly diverse in sequence and evolutionary origin, which complicates their recognition and repression. To manage this heterogeneity, cells utilize a wide array of chromatin-modifying pathways, ensuring tight control over retrotransposon activity and maintaining genomic stability, and the ChAHP complex is one of the players involved in such regulation. Retrotransposons dominate the mouse genome and include Short Interspersed Nuclear Elements (SINEs), Long Interspersed Nuclear Elements (LINEs), and Long Terminal Repeat (LTR) elements.

SINEs are non-autonomous retrotransposons, typically 100–300 base pairs in length, that rely on the enzymatic machinery of LINEs for mobilization. In the mouse genome, the most abundant SINE family are B1 and B2 elements, which are derived from tRNA or 7SL RNA sequences (Horton et al., 2023; Ichiyanagi et al., 2021; Richardson et al., 2015). Although they do not encode proteins, SINEs are often enriched in euchromatic regions and can serve as regulatory sequences and can function as binding sites for transcription factors. Interestingly, in mESCs the ChAHP complex is enriched at SINE B2 elements which also contain CTCF binding motifs (Wang et al., 2024).

LINEs are autonomous retrotransposons, approximately 6–7 kilobases in length, that encode the proteins required for their own mobilization, including a reverse transcriptase and an endonuclease. The most represented LINE family in mice is LINE-1 (L1). These elements can impact genome stability and gene regulation by generating insertions, inducing DNA double-strand breaks, and serving as sites for recombination (De Luca et al., 2023; Kemp and Longworth, 2015; Zhang et al., 2024). In addition, L1 activity has been shown to be able to interact with chromatin modifiers and, so, can influence gene expression (Percharde et al., 2018).

LTR retrotransposons are derived from endogenous retroviruses (ERVs) and are characterized by long terminal repeats at their 5’ and 3’ ends. LTR elements include families such as ERVK and ERVL. LTRs can act as strong promoters or enhancers, influencing both nearby gene expression and global chromatin organization. LTRs are silenced through DNA methylation and repressive histone marks, but during developmental processes they can remain transcriptionally active, or under stress conditions, producing regulatory RNAs or retroviral-like proteins that contribute to developmental and cellular processes (Franke et al., 2017; Lu, 2024).

ADNP interactions with HP1 and CHD4 play a crucial role in the regulation of retrotransposon. ChAHP directly binds to TE-rich genomic regions, often within euchromatic domains, and induces local chromatin compaction, thereby restricting transcription factor access and preventing aberrant TE activation. Genetic ablation of ADNP or of the ChAHP complex interactors in strictly correlated to significant deregulation of LTRs, LINEs and SINEs (Ahel et al., 2024; Ostapcuk et al., 2018).

## AIM OF THE STUDY

The goal of this study is to understand how ADNP interactions with HP1 and CHD4 govern neurodifferentiation programs. Although ADNP is well-established as a critical regulator of chromatin architecture essential for embryogenesis and brain function, the distinct roles of its individual binding partners remain poorly defined. Specifically, it is unclear how ADNP–HP1 and ADNP–CHD4 interactions contribute, either independently or cooperatively, to transcriptional repression, chromatin organization, and lineage specification during the transition from pluripotency to neuroectoderm.

This gap in understanding is especially significant given that mutations in ADNP represent one of the most common single-gene causes of autism spectrum disorders. Yet, the cellular and molecular pathways driving ADNP syndrome pathogenesis remain largely elusive.

To address this, we used in vitro models of mouse embryonic stem cells neural development that recapitulate the transition from the mESCs stage to neural progenitor cells (NPCs). This system provides a unique opportunity to dissect stage-specific functions of ADNP and the ChAHP complex during early lineage specification, while enabling integration of transcriptional, epigenomic, and nuclear organization analyses. By combining genetic perturbations of ADNP, HP1, and CHD4 with high-throughput sequencing, chromatin profiling, and imaging approaches, we aim to define the mechanistic contribution of each component to chromatin architecture, retrotransposon control, and lamina-associated domain organization. Furthermore, we seek to determine how disruption of these regulatory pathways impairs neural induction and leads to aberrant cellular states that may underlie neurodevelopmental disorders.

Ultimately, this study is designed to provide a comprehensive framework linking ADNP-dependent chromatin regulation with neural lineage commitment. By distinguishing the relative contributions of HP1- and CHD4-mediated interactions, our work will not only advance the fundamental understanding of genome regulation during early neural development but also offer mechanistic insights into the etiology of ADNP syndrome and related neurodevelopmental disorders. In the broader perspective, these findings could inform therapeutic strategies aimed at restoring proper chromatin function and improving neuronal outcomes in affected individuals.

# RESULTS

## Generation of ADNPΔCHD4 and ADNPΔHP1 separation-of-function mutants

Our first goal to examine the contribution of ADNP interactions to neurodifferentiation was to develop separation-of-function mutants where ADNP's interaction with either CHD4 or HP1 are selectively abolished. Previous reports showed that the first 228 amino acids of ADNP interact with CHD4 (Figure 2A). We examined the *Adnp* gene and determined that the coding sequence for the first 67 amino acids are contained within exons 3 and 4. Exon 5 contained the remaining coding sequence of ADNP starting with amino acid 68. Exons 4 and 5 are separated by a 2394bp intron (Figure 2B). For ease of editing and to limit the size of the genomic deletion, we excised 486bp of Adnp which results in deletion of amino acids 68 to 228 to potentially abolish CHD4 binding. We confirmed the presence of truncated ADNP in two separate clones and called these mutants "ADNPΔCHD4". The interacting region of ADNP and HP1 is more well-defined because many proteins are reported to interact with HP1 through a PxVxL motif (Lechner et al., 2005). ADNP contains the PGVLL amino acid sequence C terminus to the homeodomain, which mediates its interaction with HP1 (Figure 2A). To abolish ADNP interaction with HP1, we edited the PGVLL motif to AGSLA and called these mutants "ADNPΔHP1".

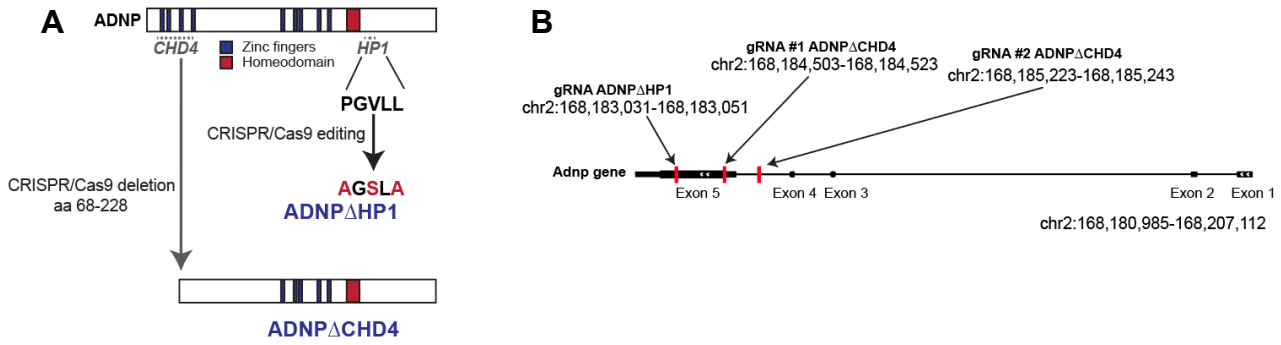


**Figure 2 CRISPR-Cas9 editing of ADNP to generate separation of function mutants.**

A) Protein schematic of mouse ADNP CRISPR-CAS9 editing. ADNPΔCHD4 strategy is indicated on the left side, ADNPΔHP1 on the right part of the scheme. B) Schematic of *Adnp* mouse gene. It is indicated exons location and gRNA localization for CRISPR-CAS9 editing for both ADNPΔHP1 And ADNPΔCHD4

Because ADNP levels are critical for neurodifferentiation of mESCs into NPCs, we first confirmed that ADNPΔCHD4 and ADNPΔHP1 are expressed at the same level as ADNP in the parental ESC lines (Figure 3). ADNP immunoprecipitation confirmed that while WT ADNP can pull down CHD4 and HP1, ADNPΔCHD4 and ADNPΔHP1 are severely

compromised for or unable to interact with CHD4 and HP1 respectively (Figures 3). Furthermore, the mutations we introduced are unlikely to give rise to broad changes in ADNP protein folding because ADNPΔCHD4 can still interact with HP1 and ADNPΔHP1 can bind CHD4 (Figures 3).

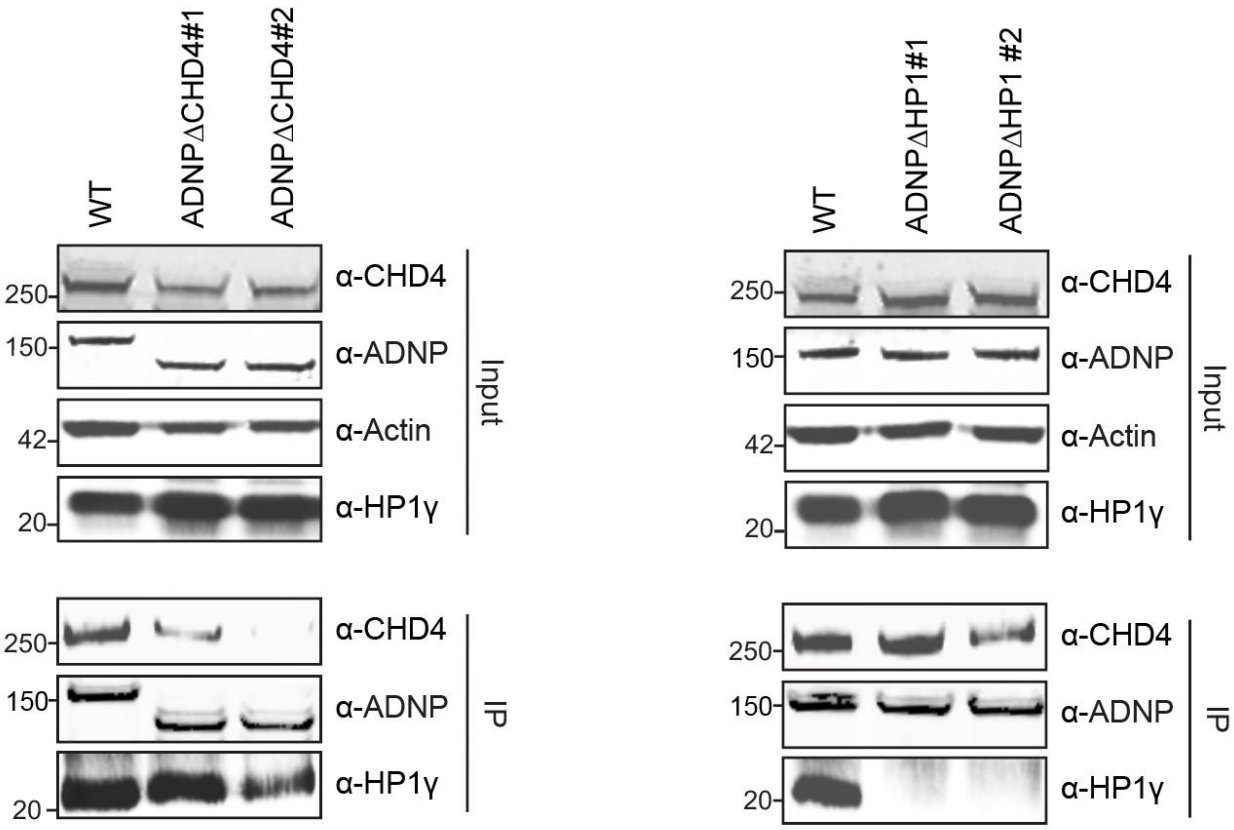


**Figure 3 Mutants are defective for ADNP-HP1 or ADNP-CHD4 interaction.**

Western blot for ADNP IP (bottom) and Input (top) in ADNPΔHP1 (left) and ADNPΔCHD4 (right). MW are indicated on the left and antibodies on the right.

## ADNP-HP1 interactions are essential for neurodifferentiation

In vitro models of mammalian development have demonstrated that the progression from ESCs to neural progenitor cells (NPCs) is not direct but occurs through a transient intermediate state known as the epiblast-like cell (EpiLC). ESCs maintained in culture resemble the naïve pluripotent state of the pre-implantation inner cell mass, characterized by the expression of factors such as Nanog, Esrrb, Klf4, and Rex1, and by an open chromatin landscape permissive to multiple lineage options (Brook and Gardner, 1997; Kalkan et al., 2017; Nichols and Smith, 2009). In contrast, EpiLCs capture the primed

pluripotent state of the post-implantation epiblast, which has undergone partial lineage restriction while retaining developmental potential. The transition from ESCs to EpiLCs can be induced by fibroblast growth factor (FGF) and Activin/Nodal signalling, which repress naïve pluripotency regulators and activate transcription factors including Otx2, Oct6, and Zic2 that are characteristic of primed pluripotency (Buecker et al., 2014; Kalkan and Smith, 2014).

EpiLCs represent a critical window of competence for lineage specification. When exposed to inhibitory signals that suppress BMP, Wnt, and TGF-β pathways, EpiLCs are efficiently directed toward a neuroectodermal fate (Kalkan and Smith, 2014; Marks et al., 2012). Neural induction at this stage is accompanied by the activation of early neural markers such as Sox1, Sox2, and Pax6, and by the establishment of neural progenitor identity (Pevny and Placzek, 2005; Zhang et al., 2010). The transition from EpiLC to NPC involves both transcriptional reprogramming and chromatin reorganization, including the resolution of bivalent promoters at developmental genes, the deposition of H3K27ac at neural enhancers, and the repositioning of neural loci into transcriptionally active nuclear compartments (DeGroat et al., 2024; Kishi and Gotoh, 2018). NPCs generated through this stepwise progression display characteristic features of early neuroepithelium, including a polarized epithelial morphology, self-renewal capacity, and the ability to differentiate into neurons and glial cells under appropriate conditions. This ESC–EpiLC–NPC paradigm has become a widely used in vitro system for dissecting the molecular logic of neural lineage specification and for modelling the earliest stages of mammalian neurodevelopment.

We used a differentiation protocol to differentiate mESCs to NPCs (Gouti et al., 2014). We differentiated two independent ADNPΔCHD4 or ADNPΔHP1 clones alongside WT and ADNP knockout (ADNP KO) mESCs. As expected at the end of the differentiation experiment, WT mESCs formed NPCs as was evident by the formation of long neurite like extensions in culture (Figure 4). As previously shown, ADNP KO mESCs were severely compromised in their ability to neurodifferentiate (Figure 4) (Ostapcuk et al., 2018; Yan et al., 2022). While ADNP KO differentiated similar to WT until the EpiLC stage (Figure 5), they began exhibiting signs of cell death upon transitioning from EpiLCs to NPCs. Similarly, both ADNPΔCHD4 and ADNPΔHP1 appeared identical to WT at the EpiLC stage.

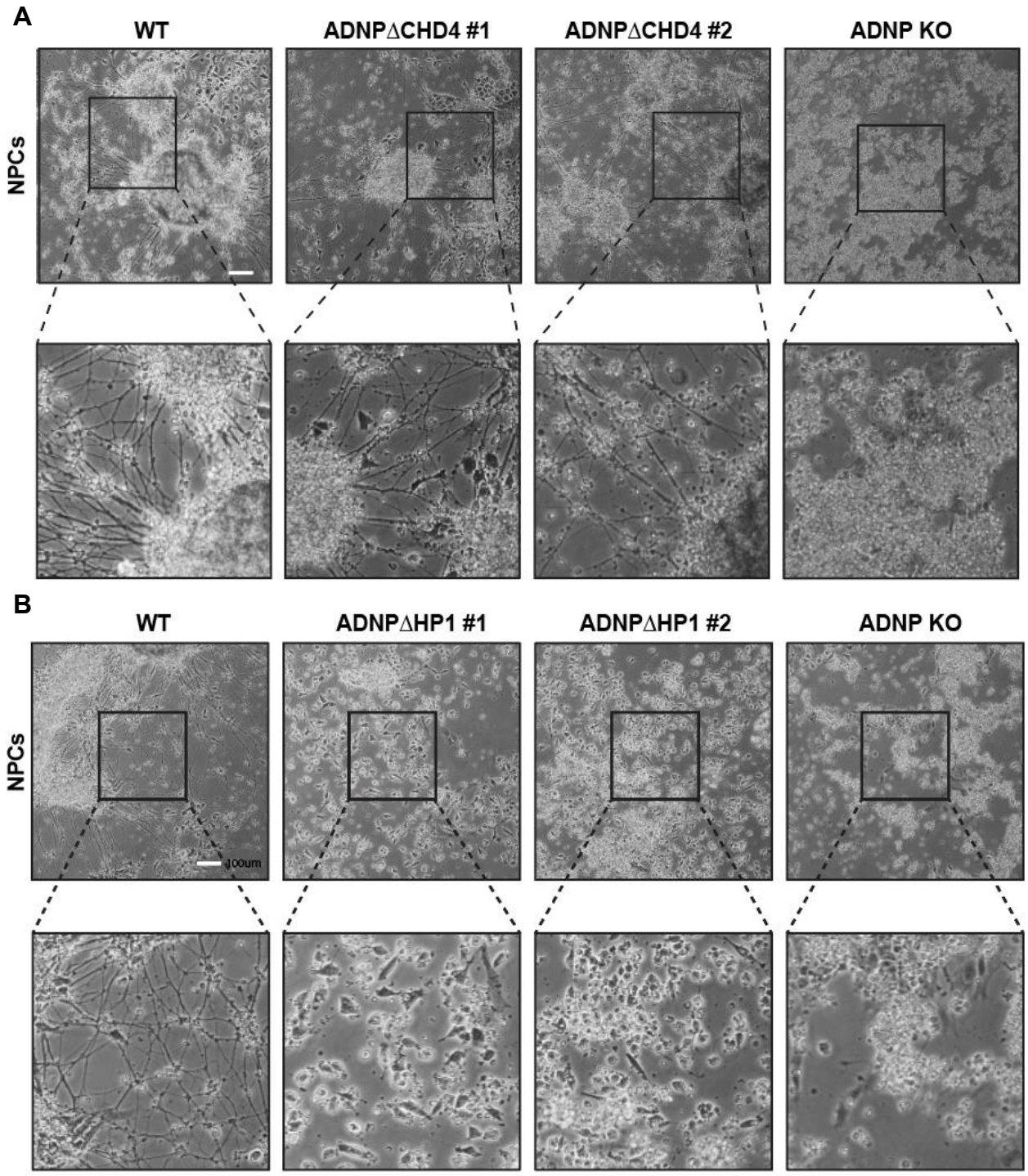


**Figure 4 HP1-ADNP, but not CHD4-ADNP, is required for correct neural specification.**

Representative images of WT, ADNP KO and ADNPΔCHD4 (A) or ADNPΔHP1 (B) cells on day 6 of neural differentiation.

However, ADNPΔHP1, but not ADNPΔCHD4, began to resemble ADNP KO after exit from the EpiLC stage and failed to form NPCs (Figure 4). We conclude that ADNP interactions with HP1 are vital for differentiation of ESCs to NPCs.

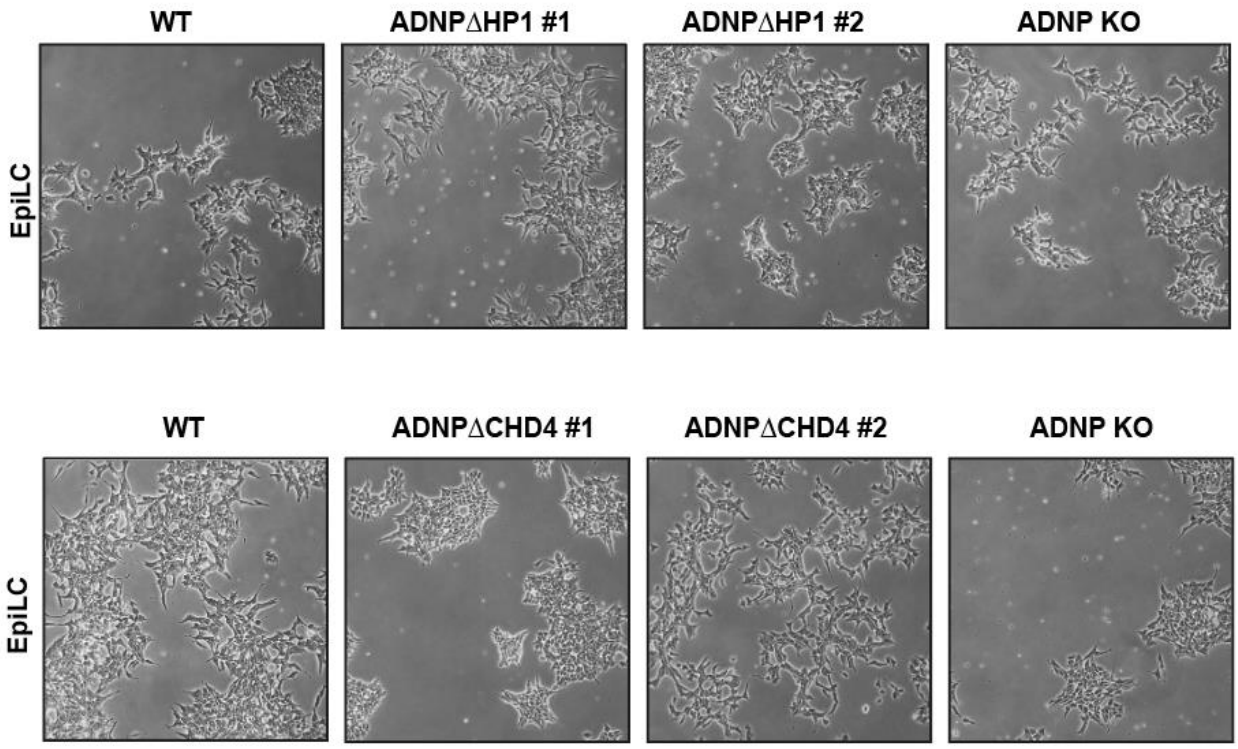


**Figure 5 HP1 and CHD4 interactions are not required for early step of differentiation.**

Representative images of WT, ADNP KO and ADNPΔHP1 (top) or ADNPΔCHD4 (bottom) cells on day 2 of neural differentiation, at the Epiblast-like cells stage.

### HP1 and CHD4 drive ADNP on different genomic regions

At most sites, ADNP interaction with chromatin determines the localization of HP1 and CHD4 (Ostapcuk et al., 2018). However, at some specific heterochromatin regions, such as long terminal repeats (LTRs) and Long interspersed elements (LINEs) retrotransposons, which are enriched for histone H3 lysine 9 (K9) methylation and bound by HP1, ADNP localization is dependent on HP1 interactions (Ahel et al., 2024). We examined how ADNP localization is affected genome wide when it is unable to interact with HP1 or CHD4. We performed ADNP CUT&RUN in WT, ADNPΔCHD4, and ADNPΔHP1 and identified 20,786 peaks that we defined as ADNP binding sites in mESCs. Overall, while ADNP localizes similarly across most ADNP target sites (Figure 6A) in both mutants, we observed that ADNPΔCHD4 showed a slight decrease in ADNP signal across all these sites. A potential reason for this is that ADNPΔCHD4 was generated by a deletion that removed the first 4 zinc fingers of ADNP, which may help stabilize ADNP binding to chromatin. Differential binding analysis revealed that while ADNP localization was not changed at the majority of sites in ADNPΔHP1, 1,301 genomic regions showed significant changes in ADNP localization. Of these, 440 regions gained ADNP, and 861 regions lost ADNP in ADNPΔHP1 mESCs (Figure 6B, 6C). Similar

analysis of ADNP localization in ADNPΔCHD4 mESCs compared to WT mESCs identified a total of 2,020 regions with altered ADNP, with 1,506 sites gaining and 514 sites losing ADNP (Figure 6B, 6C). Importantly, most of the gained and lost ADNP sites are unique between the two mutants, with 60 shared gained sites and 17 shared lost sites, suggesting distinct roles for HP1 and CHD4 interactions in ADNP targeting to the genome (Figure 6D).

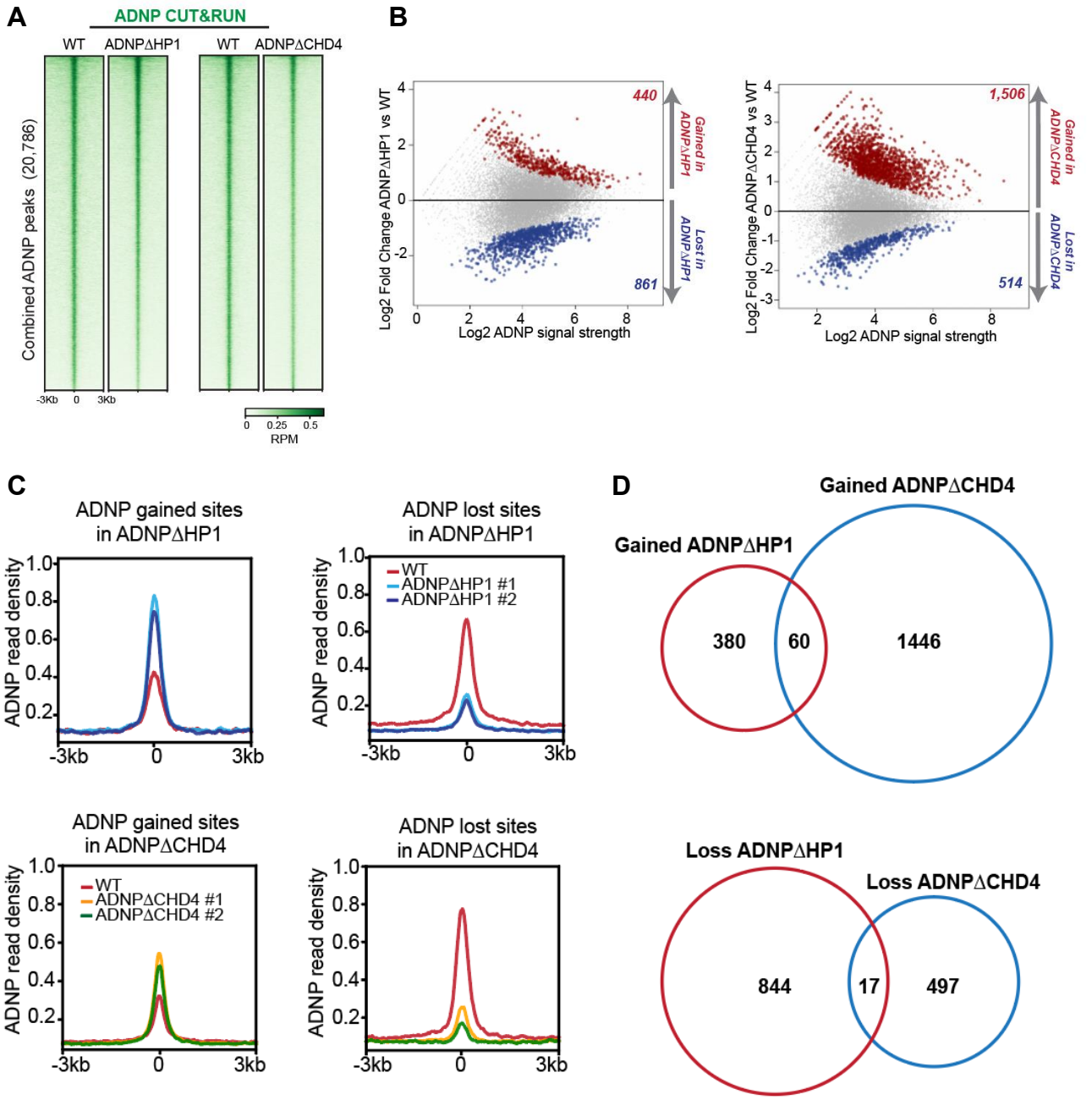


**Figure 6 HP1 and CHD4 drive ADNP on different genomic regions.**

A) Heatmap of ADNP CUT&RUN signal in WT, ADNPΔHP1 and ADNPΔCHD4 across 6-kb windows centered on ADNP CUT&RUN peaks. Signal is RPM. B) MA plot of ADNP signal in significant differential ADNP sites (FDR < = 0.05, DiffBind). ADNPΔHP1 vs WT (left, 440 gained in red, 861 lost in blue) and ADNPΔCHD4 vs WT on the right (1506 gained in red, 514 lost in blue). C) ADNP signal density on gained and lost sites in ADNPΔHP1 (top) and ADNPΔCHD4 (bottom). D) Overlap of gained (top) and lost (bottom) sites from ADNPΔHP1 and ADNPΔCHD4.

Further examination of the genomic features that gain or lose ADNP when it cannot interact with HP1 revealed that ADNP is mainly gained at promoters and lost from intergenic sites (Figure 7A). The regions which lose ADNP in ADNPΔHP1 are enriched for H3K9me3 (ENCODE, 2012) (Figure 7B,C) that contain heterochromatic retrotransposons such as LTRs (Figure 7D). ADNPΔHP1 is gained at genomic sites that already contain ADNP and are low in H3K9me3 and likely where the ChAHP complex is recruited to chromatin through HP1 independent interactions (Figure 7B,C).

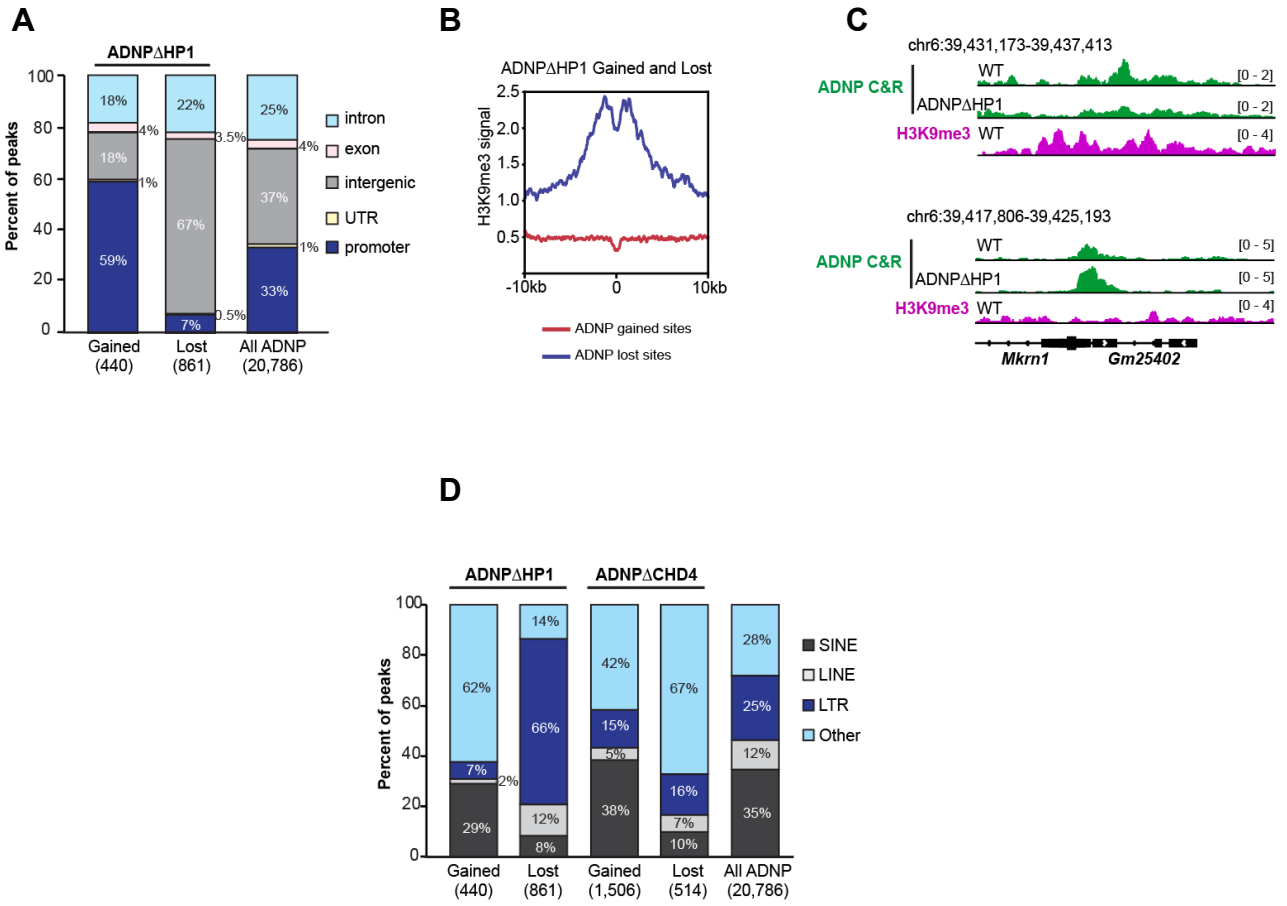


**Figure 7 ADNPΔHP1 gained and lost sites features.**

A) Bar plot annotation of gained and lost sites in ADNPΔHP1. B) H3K9me3 signal on gained and lost sites in ADNPΔHP1. C) Genome browser view (right) of one gained (top) and one lost (bottom) sites in ADNPΔHP1. The browser shot is showing ADNP CUT&RUN signal (RPM) in WT mESC and in ADNPΔHP1 and H3K9me3 ChIP signal in WT mESC. D) Bar plot for transposable elements overlaps with gained and lost sites in ADNPΔHP1 and ADNPΔCHD4 mutant.

In contrast, ADNP localization changes in ADNPΔCHD4 were distinct from ADNPΔHP1 and not as skewed toward a specific genomic feature. In ADNPΔCHD4, ADNP was gained at intergenic and intronic sites, and lost from promoters (Figure 8A) and show reduced

H3K9me3 (Figure 9B). To gain further insight on the regions that gain or lose ADNP in ADNPΔCHD4, we used an X state ChromHMM model to discover specific characteristics of these genomic regions. We found that ADNPΔCHD4 was specifically gained at CTCF sites (Figure 8C,D). In contrast, ADNP was lost at genomic sites that did not show CTCF enrichment (Figure 8D).

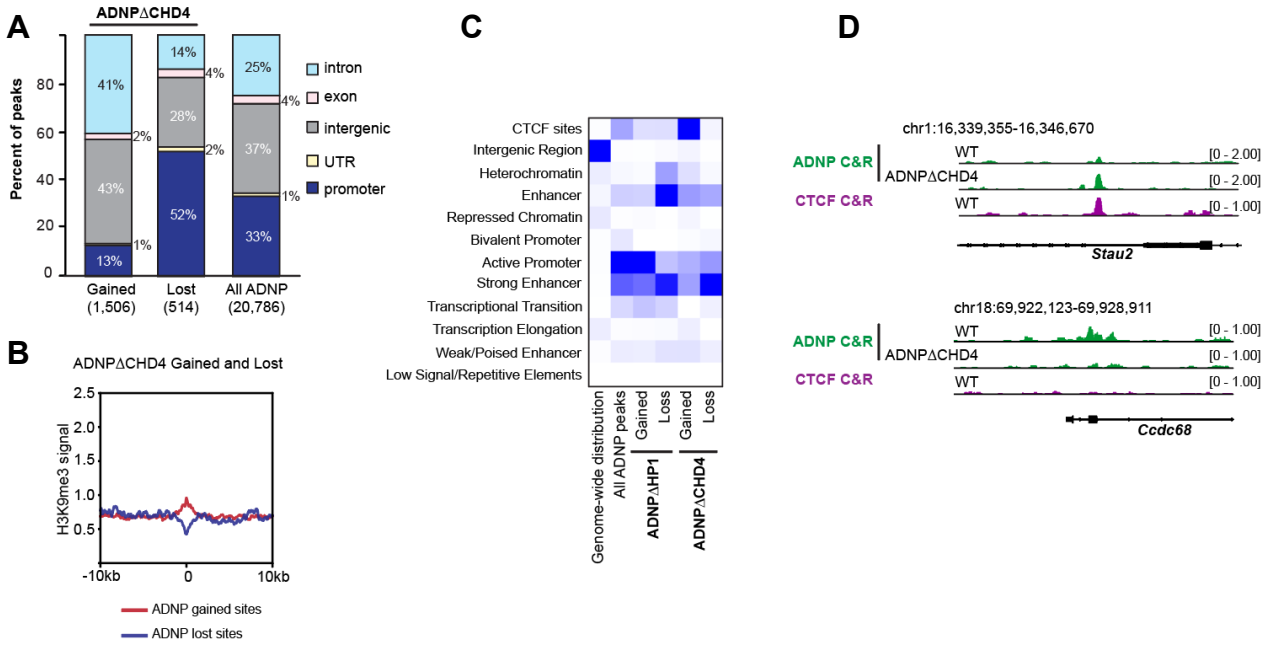


**Figure 8 ADNPΔCHD4 gained and lost sites features.**

A) Bar plot annotation of gained and lost sites in ADNPΔCHD4. B) H3K9me3 signal on gained and lost sites in ADNPΔCHD4. C) ChromHMM analysis of gained and lost sites in ADNPΔHP1 and ADNPΔCHD4. D) Genome browser view (right) of one gained (top) and one lost (bottom) sites in ADNPΔHP1. The browser shot is showing ADNP CUT&RUN signal (RPM) in WT mESC and in ADNPΔHP1 and CTCF CUT&RUN signal in WT mESC.

Global CTCF occupancy was not significantly changed in either ADNPΔHP1 or ADNPΔCHD4 (Figure 9A), but we found an increase in CTCF signal when we looked at a subset of genomic regions that were gained by CTCF in ADNP KO analysis from a previously published dataset from our lab (Figure 9B) (Wulfridge et al., 2023). Interestingly, these regions that result in CTCF accumulation are enriched for Sine B2 elements (Figure 9C). Our data indicates that ADNP interactions may play a role in preventing CTCF occupancy at SINE B2-enriched regions. In particular, ADNP interactions with CHD4 may contribute to CTCF occupancy at specific sites, but this function is not critical for early neurodifferentiation.

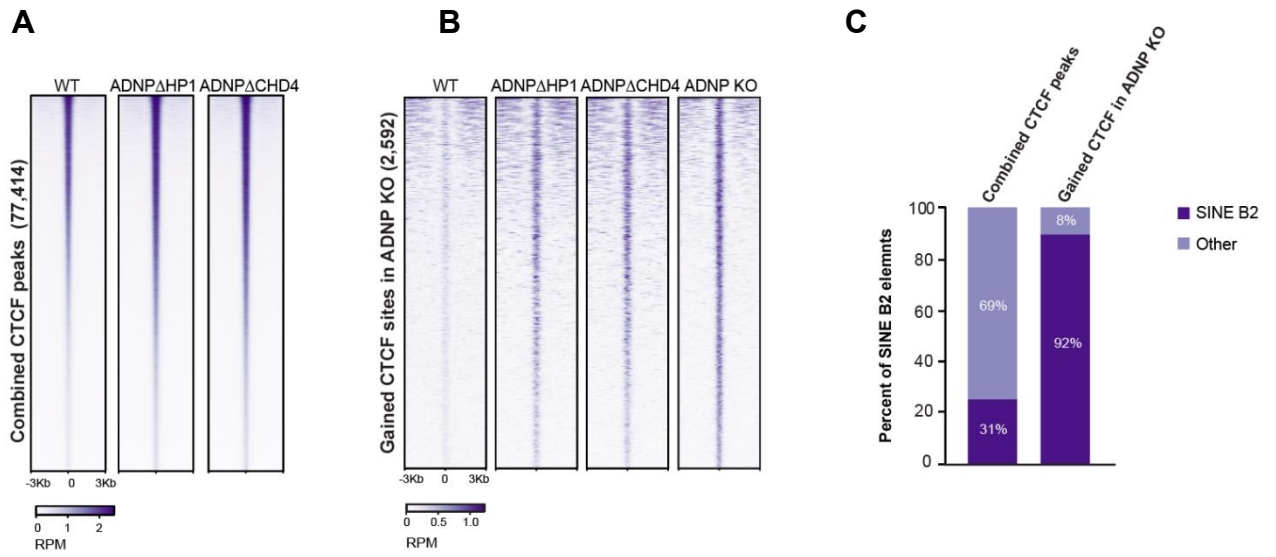


**Figure 9 ADNPΔHP1 and ADNPΔCHD4 displayed changes in CTCF binding.**

A) CTCF CUT&RUN signal (RPM) in WT, ADNPΔHP1 and ADNPΔCHD4 cells. Signal is centered on a 6kb windows over CTCF peaks. B) CTCF CUT&RUN signal (RPM) in WT, ADNPΔHP1, ADNPΔCHD4 and ADNP KO cells. Signal is centered on a 6kb windows over CTCF gained peaks in ADNP KO. C) Barplot showing enrichment for SINE B2 elements over all CTCF peaks or gained CTCF peaks in ADNP KO.

**ADNP loss at pericentromeres derepresses major satellites despite presence of HP1**

Our data indicate that disrupting the ADNP-HP1 interaction leads to significant defects in differentiation towards neural fate. Previous characterization of the ChAHP complex showed that ADNP deletion resulted in the loss of HP1 and CHD4 at many genomic regions (Ostapcuk et al., 2018). These results suggest that ADNP determines the localization of HP1 and CHD4 at most sites. However, at some specific heterochromatin regions, such as long terminal repeats (LTRs), Long interspersed nuclear elements (LINEs) retrotransposons, and pericentromeres, which are enriched for histone H3 lysine 9 (K9) methylation and bound by HP1, ADNP localization is dependent on HP1 interactions (Ahel et al., 2024; Mosch et al., 2011). We examined the localization of ADNP in WT, ADNPΔHP1, and ADNPΔCHD4 mESCs. We found that ADNP was enriched at pericentromeres in WT mESCs (Figure 10) and was completely lost from these regions in ADNPΔHP1 (Figure 10) confirming previous results from overexpression studies (Mosch et al., 2011). In ADNPΔCHD4, many cells still showed ADNP presence at pericentromeres, however their levels were slightly lower than in WT mESCs (Figure 10), suggesting that CHD4 function may be important for stable association of ADNP to these regions.

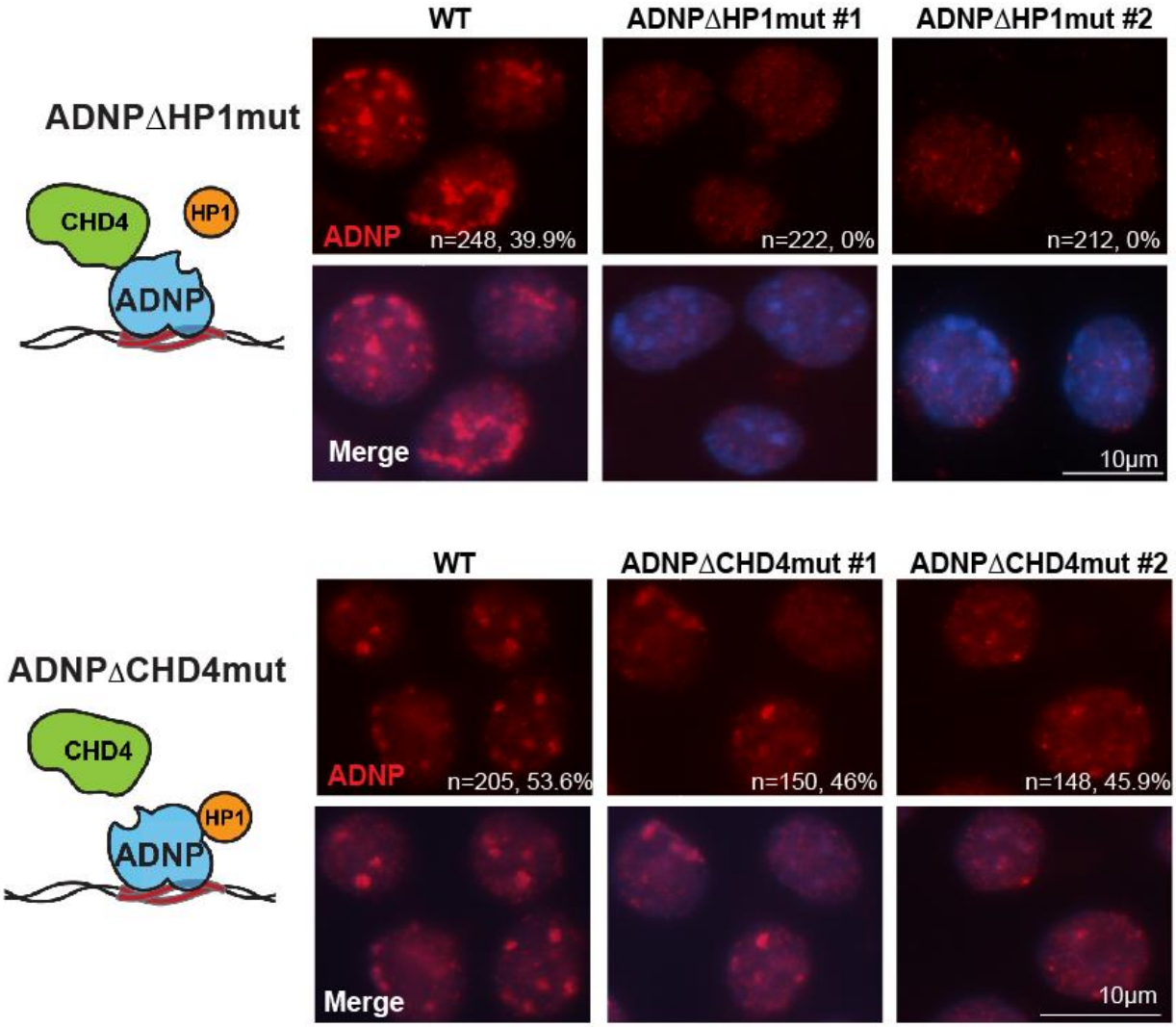


**Figure 10 HP1, but not CHD4, is required for ADNP localization at pericentromeres.**

Representative images showing subcellular localization of ADNP (red) in WT mESC and two ADNPΔHP1 clones (top) or two ADNPΔCHD4 clones (bottom). Nuclei are stained with DAPI (blue). Represented is the percentage of cells showing ADNP enrichment at pericentromeres.

HP1γ enrichment at pericentromeres was similar in WT, ADNPΔHP1, and ADNPΔCHD4 (Figures 11A,C). Finally, CHD4 localization in ADNPΔHP1, and ADNPΔCHD4 also mimicked WT mESCs (Figure 11B,D).

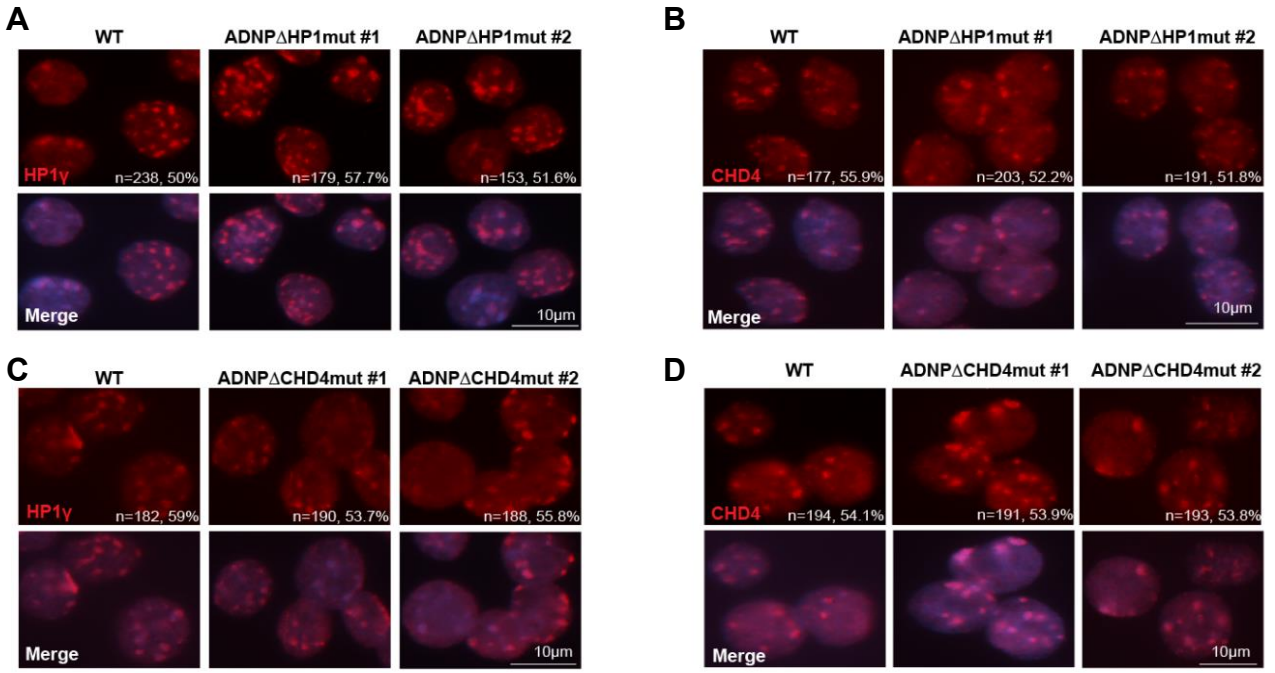


**Figure 11 HP1 and CHD4 localization at pericentromeres is not affected by ADNP interactions.**

Representative images showing subcellular localization of HP1γ (A, B) or CHD4 (C, D) in WT mESC and two ADNPΔHP1 clones (top) or ADNPΔCHD4 clones (bottom). Nuclei are stained with DAPI (blue). Represented is the percentage of cells showing HP1γ enrichment over pericentromeres in each sample.

To determine whether loss of ADNP influenced pericentromeres organization, we employed STORM super-resolution fluorescence microscopy of major satellite repeats to gain a more detailed understanding of the structural alterations occurring at pericentromeric heterochromatin. Cells were processed following standard DNA-FISH procedures using an Alexa647-conjugated major satellite repeat probe and Hoechst counterstaining. Quantitative cluster analysis of the STORM data was then performed to define individual major satellite repeat clusters and calculate their mean signal density (Figure 12A). This analysis revealed a significant decrease in average major satellite signal density in ADNPΔHP1, whereas both ADNPΔCHD4 and KO showed increased values (Figure 12B). A reduction in signal density reflects decreased local DNA compaction, as lower fluorophore density corresponds to a more relaxed chromatin configuration (Martin et al., 2021; Otterstrom et al., 2019). Therefore, the observed reduction in density in ADNPΔHP1 confirms a pronounced pericentromeric decondensation phenotype. Conversely, we observed an unexpected increase in major satellite signal density in ADNPΔCHD4 and ADNP KO.

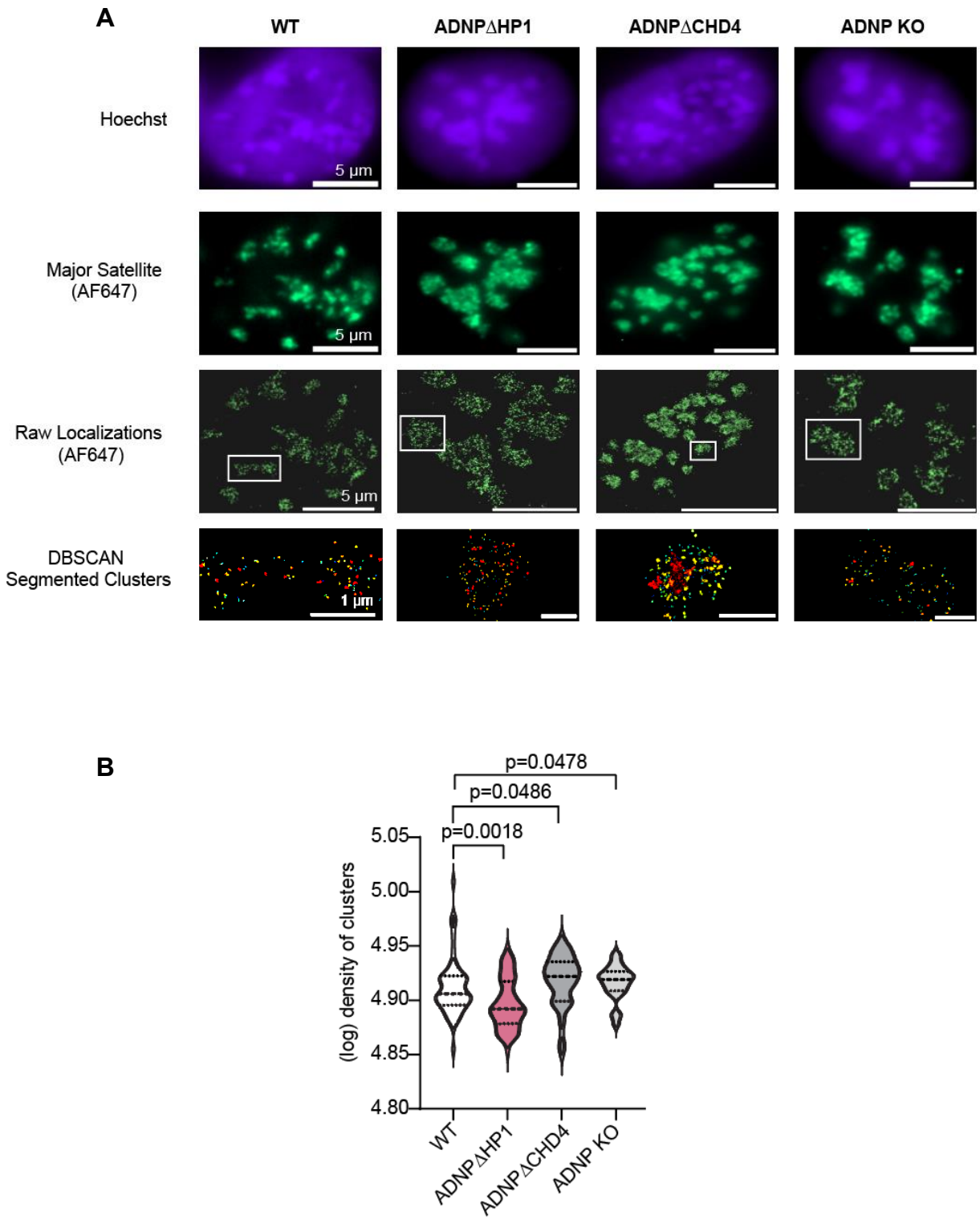


**Figure 12 HP1-ADNP is required to maintain pericentromeric architecture**

A) Representative images showing MSR DNA localization (AF647) in WT, ADNPΔHP1, ADNPΔCHD4 and ADNP KO mESCs. First row shows Hoechst staining; second row shows confocal images for single cell. Raw localizations (AF647) images are STORM acquired, displaying DNA-FISH staining for MSR. DBSCAN row show segmentation analysis of clusters based on area of the nuclear region inside the white rectangle. B) Violin plot showing mean cluster densities from STORM analysis of WT, ADNPΔHP1, ADNPΔCHD4 and ADNPKO mESCs.

Pericentromeres consists of repetitive sequences found in the pericentromeric regions of chromosomes. ADNP localization at pericentromeres through HP1 was demonstrated to be critical for silencing Major Satellite Repeats(MSR) (Mosch et al., 2011). To assess whether ADNP interactions with HP1 or CHD4 contribute to major satellite silencing, we performed RNA-seq on our mutants and evaluated the expression of major satellite repeats. Interestingly, ADNP-mediated repression of major satellite repeats was alleviated by the disruptions of both CHD4 and HP1 interactions. In line with the decondensation phenotype observed in ADNPΔHP1, these mutants exhibited a greater upregulation of major satellite transcripts compared to ADNPΔCHD4 (Figure 13A,B). This hypothesis was supported by the analysis of nuclear area changes across mutants. The swarm plot in Figure 13C showed a significant increase in nuclear area for the ADNPΔHP1 mESCs. Together, we conclude that ADNP interactions with both HP1 and CHD4 are important for repression of major satellite repeats, although this shared effect does not explain why only ADNPΔHP1, and not ADNPΔCHD4, exhibits neurodifferentiation defects.

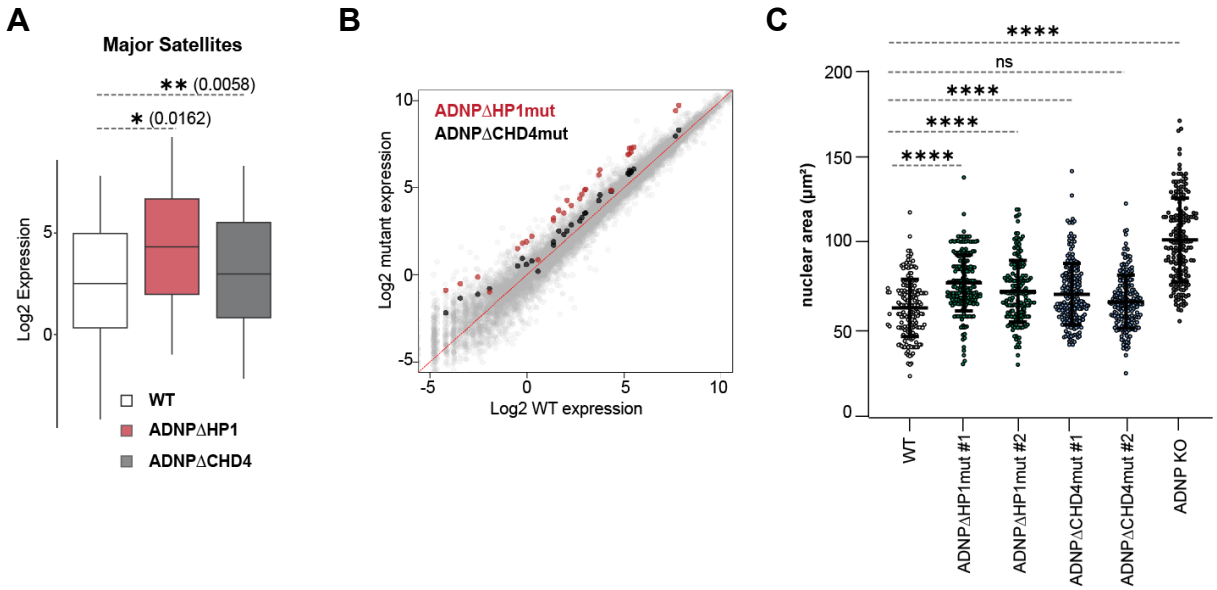


**Figure 13 HP1 and CHD4 are required for Major Satellite repression**

A) Boxplot displaying log2 expression of Major Satellite transcripts in WT mESC (white), ADNPΔHP1 (red) and ADPΔCHD4 (grey). P-values are calculated with paired t-test. B) Plot showing Log2 average expression of MSR transcripts in WT and ADNPΔHP1 or ADNPΔCHD4 mutants. C) Swarm plot showing distribution of nuclei areas in WT, ADNPΔHP1, ADNPΔCHD4 and ADNP KO cells.

**HP1 and CHD4 interaction with ADNP repress transposable elements**

The ChAHP complex plays a role in repression of retrotransposons. Consistent with this, ADNP deletion results in upregulation of SINE B2 elements, LINE elements, and LTRs (Ahel et al., 2024; Kaaij et al., 2019). Interestingly, ADNP localizes to heterochromatic retrotransposons such as LTRs and LINEs through its interaction with HP1. We examine retrotransposon derepression in ADNPΔHP1 and ADNPΔCHD4 to determine if ADNPΔHP1 showed greater deregulation of transposable elements which would contribute to genome instability and neurodifferentiation defects. We found that both ADNPΔHP1 and ADNPΔCHD4 mESCs showed deregulation of LINEs, SINEs and LTRs (Figure 14A,B). Surprisingly, ADNPΔCHD4 showed larger numbers of LTRs that were deregulated compared to ADNPΔHP1 (329 in ADNPΔHP1 and 480 in ADNPΔCHD4). Similarly, a larger number of LINEs and SINEs were deregulated in ADNPΔCHD4 (431 LINEs and 289 SINEs in ADNPΔHP1 compared to 808 LINEs and 549 SINEs in ADNPΔCHD4). Therefore, taken together with our data showing that ADNPΔCHD4 mESCs can differentiate into NPCs, retrotransposon reactivation may not contribute to cell death during neurodifferentiation.

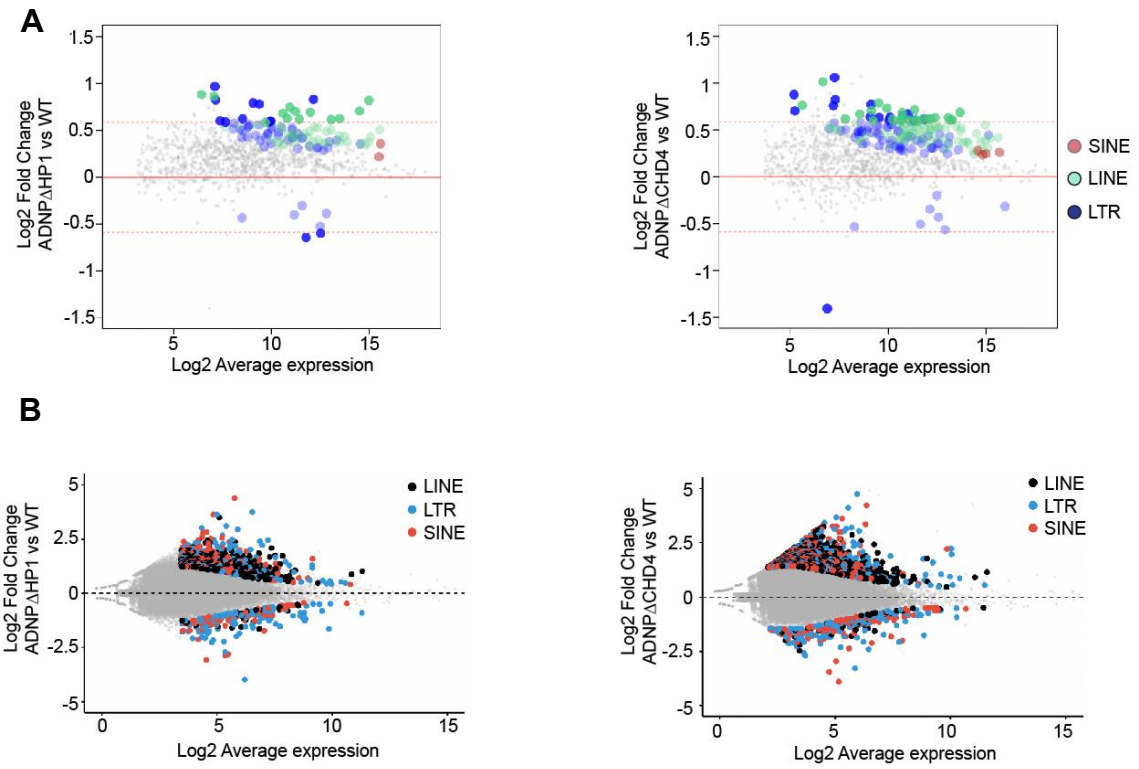


**Figure 14 The ChAHP complex regulate transposable elements transcription.**

A) MA plot for SINEs, LINEs and LTRs fold change grouped by subfamilies group fold change in ADNPΔHP1 vs WT (left) or ADNPCHD4 vs WT (right). B) MA plot for each SINEs, LINEs and LTRs fold change in ADNPΔHP1 vs WT (left) or ADNPCHD4 vs WT (right).

**ADNP is lost from Lamin associated domains in ADNPΔHP1**

Spatial organization of chromatin plays an important role in gene regulation (Ghosh and Meyer, 2021). Heterochromatin and silent genes are frequently localized to the nuclear periphery. Because of the unique effect of ADNPΔHP1 on neurodifferentiation, we examined other regions of the genome where ADNP localization may be regulated through its interaction with HP1. Heterochromatin is organized at the nuclear periphery and interacts with nuclear lamina. These Lamin associated domains (LADs) are enriched for heterochromatic histone marks such as H3K9me2/3, H3K27me3 and HP1 proteins (Martin et al., 2025; Shah et al., 2023; Ye and Worman, 1996). Using a published dataset for LADs in mESC (Peric-Hupkes et al., 2010), we found that the majority of sites that lose ADNP in ADNPΔHP1 overlap with LTRs (Figure 7A) and almost 30% of these are localized to LADs (Figure 15A). Examination of ADNP localization at LAD targets versus other regions confirmed that ADNP is specifically lost at LADs in ADNPΔHP1, but not in ADNPΔCHD4 (Figure 15B,C). Recently, different labs demonstrated the positive correlation between genes length and biological functions. Longer genes tend to be often associated with neuronal development and, in general, with early developmental stages (Lopes et al., 2021; McCoy and Fire, 2020; Takeuchi et al., 2018; Zylka et al., 2015). Longer genes present are prone to be more challenging to regulate due to their complex structure and transcriptional demands, leading to biases that may influence gene expression efficiency and vulnerability to transcriptional errors, potentially contributing to neural disease mechanisms (Khandia et al., 2022; Takeuchi et al., 2018). Interestingly, we observed a marked increase in the average gene length among genes identified as ADNP targets at LADs (Figure 15D), suggesting a potential tendency of ADNP to preferentially associate with long neural genes at heterochromatin regions.

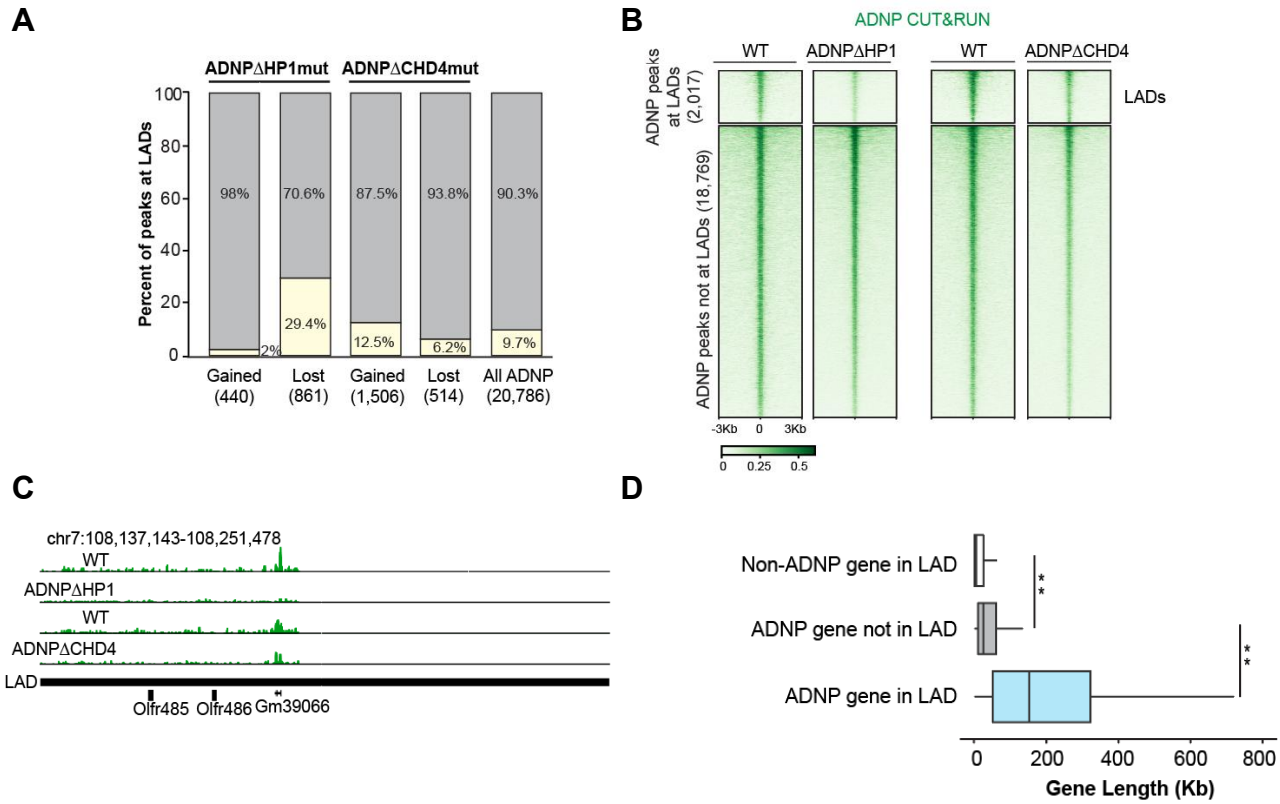


**Figure 15 HP1 mediates ADNP localization LADs.**

A) Barplot for showing percentages of ADNP peaks localizing at LADs for gained and lost ADNP sites. B) Heatmap of ADNP CUT&RUN signal in WT, ADNPΔHP1 and ADNPΔCHD4 across 6-kb windows centered on ADNP CUT&RUN peaks. Peaks are clustered based on localization at LADs (top) or not (bottom). Signal is RPM. C) Browser view showing ADNP signal from CUT&RUN at a representative LADs. D) Bar plot showing average gene length of gene sets.

Next, we examined the expression of ADNP targets which localize to LADs in ADNPΔHP1. We performed QuantSeq in WT mESC, ADNPΔHP1 and ADNPΔCHD4 to found that a number of ADNP target genes that are silent or expressed at very low levels and localized to LADs in WT mESCs are upregulated in ADNPΔHP1 (Figure 16A), while they showed no changes in ADNPΔCHD4. Specific proteins play a role in tethering chromatin to nuclear lamina. HP1 proteins play a key role in connecting heterochromatin to the nuclear lamina, thereby contributing to nuclear structural integrity. By directly interacting with LBR, an integral membrane protein of the inner nuclear membrane, HP1 helps anchor heterochromatin at the nuclear periphery in higher eukaryotic cells (Ye et al., 1997). HP1 not only maintains nuclear mechanical stability during interphase but may also facilitate dynamic reorganization of chromatin and the nuclear envelope throughout the cell cycle (Polioudaki et al., 2001; Sanulli et al., 2019; Ye and Worman, 1996). In such context, our results

suggested that HP1γ could play a crucial role in localizing ADNP at LADs in order to correctly regulate the expressions of genes involved in neural development during the early stage of differentiation.

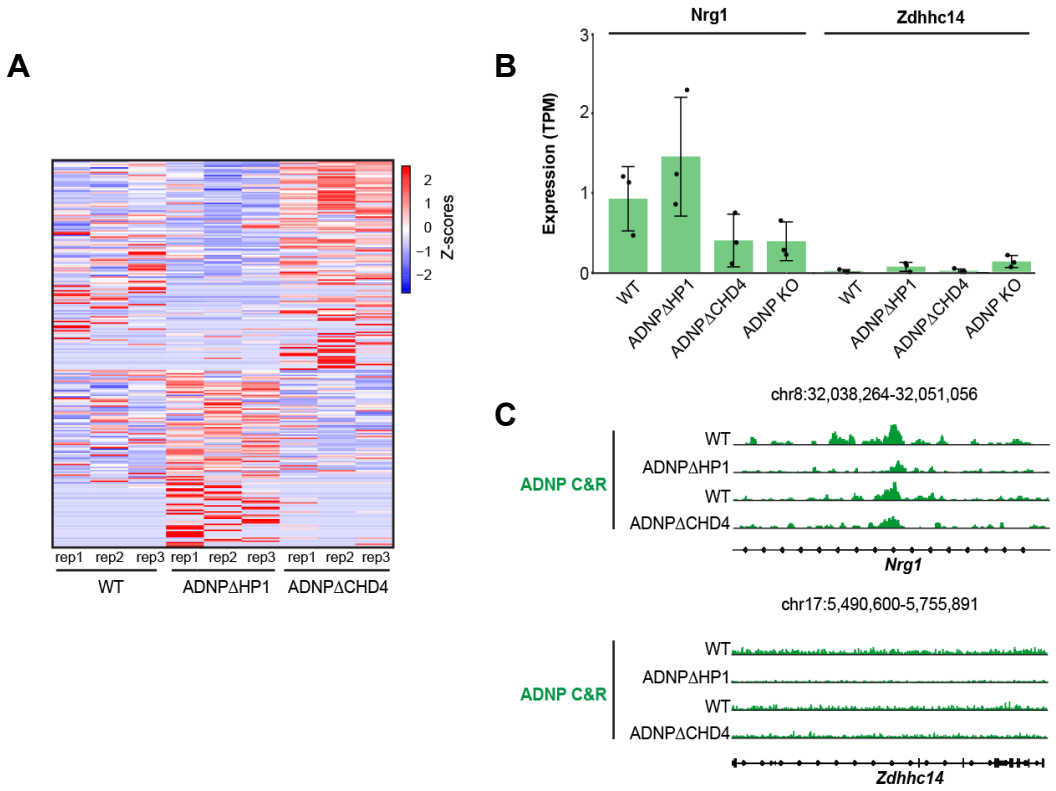


**Figure 16 ADNP target genes at LADs are differentially expressed in mutants.**

A) Heatmap showing z-scores values for expression of ADNP target genes at LADs. B) TPM expressions for representative genes in WT, ADNPΔHP1, ADNPΔCHD4 and ADNP KO. It is showed an ADNP target at LADs (Nrg1, left) and a control gene (Zdhhc14, right) C) Browser view for ADNP CUT&RUN signal on genes from Fig. 17B. Tracks indicates ADNP signal in WT, ADNPΔHP1 and ADNPΔCHD4.

To further explore the role of ADNP in organizing chromatin at the nuclear periphery through HP1, we examined whether loss of ADNP interactions affects the spatial positioning of its target genes relative to the nuclear lamina. Cells were stained with an anti-Lamin B1 antibody and subjected to DNA FISH using probes for three ADNP target genes located within LADs (Nrg1, Fggy, and Tcf12), which were upregulated in the ADNPΔHP1 mutant and showed reduced ADNP binding across their gene bodies (Figure 16 B,C). As controls, we included three genes not associated with LADs (Zdhhc14, Col2a1, and Ccn5). Dual-color FISH was performed to simultaneously visualize one target and one control gene in wild-type, ADNPΔHP1, ADNPΔCHD4, and ADNP knockout cells. The distance of each locus from the Lamin B1-stained nuclear envelope was measured and plotted as a relative frequency distribution against the distance from the nuclear periphery (Figure 17A,B). Remarkably, no

significant changes were detected in the positioning of either target or control genes, indicating that the overall spatial organization of these loci at the nuclear periphery remains unaltered in ADNP mutant cells (Figure 17 A,B).

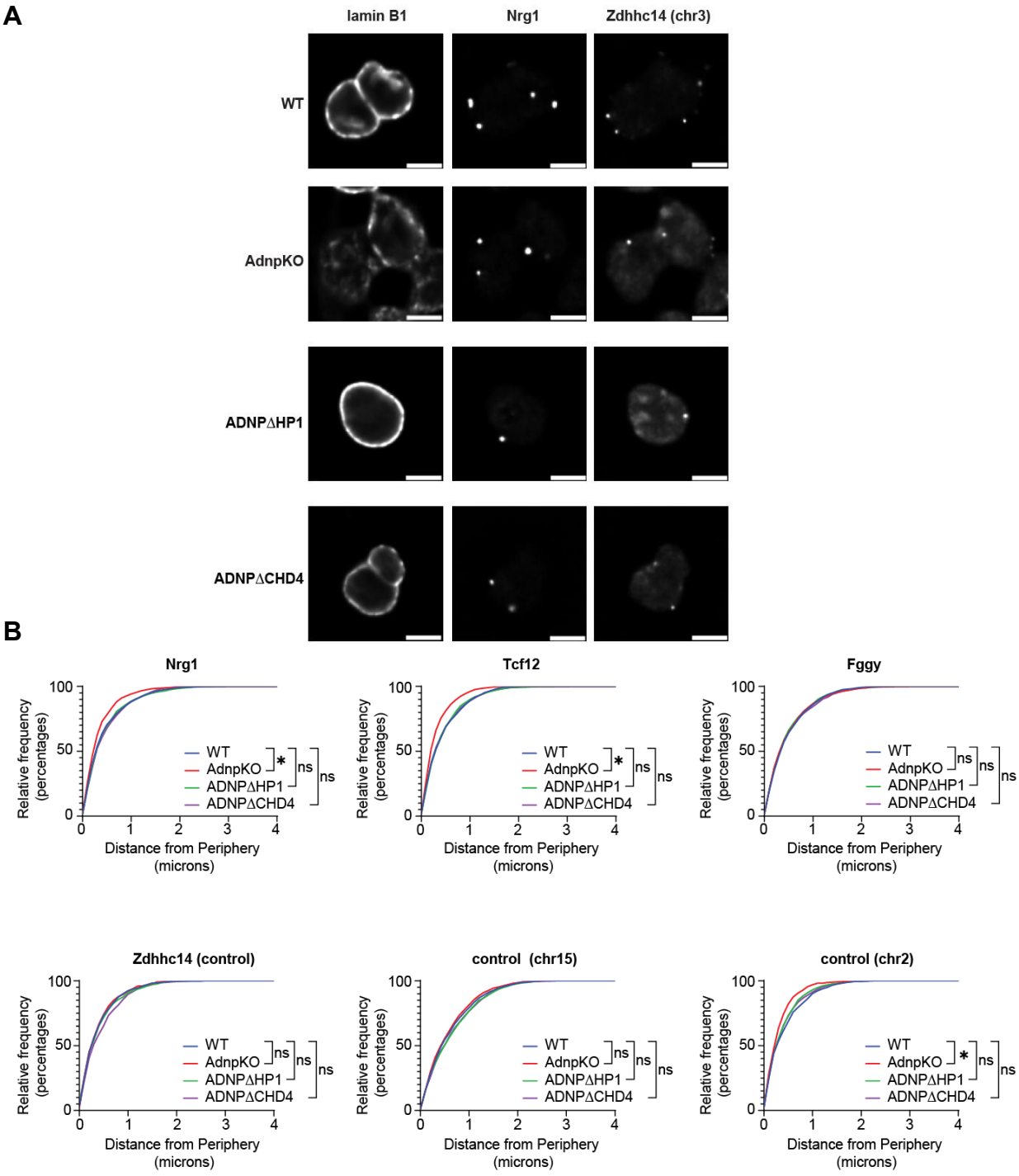


**Figure 17 ADNP-HP1 disruption doesn't impact gene localization at LADs.**

A) Representative images of DNA-FISH and LaminB1 staining in WT, ADNPΔHP1, ADNPΔCHD4 and ADNP KO mESC. Here it shown staining for LmnB1, Nrg1 (ADNP target gene at LADs) and Zdhhc14 (control, not ADNP target). B) Curves showing average distance of 3 ADNP target genes at LADs (top) and 3 control genes (bottom) in WT, ADNPΔHP1 , ADNPΔCHD4 and ADNP KO.

As previously shown, ADNP is lost from LADs upon destabilization of its interaction with HP1. To explore the functional consequences of ADNP redistribution from LADs, we identified ADNP target genes within LADs that were upregulated, defined as showing at least a twofold increase in expression, in both ADNPΔHP1 and ADNPΔCHD4 mutants compared to wild-type cells. We then examined the overlap between these upregulated gene sets, revealing 33 shared genes, 52 unique to ADNPΔHP1, and 45 unique to ADNPΔCHD4 (Figure 18). To gain insight into their biological roles, we performed Gene Ontology (GO) Biological Process analysis separately on the HP1-only and CHD4-only upregulated gene sets. GO analysis revealed that genes upregulated specifically in ADNPΔHP1 were enriched for neural-related processes such as nervous system development and synaptic signaling, suggesting that the ADNP–HP1 interaction plays a key role in repressing neural genes within heterochromatin (Figure 18). In contrast, genes upregulated only in ADNPΔCHD4 were associated with growth factor and receptor signaling pathways, pointing to a distinct regulatory function for the ADNP–CHD4 interaction. These findings suggest that ADNP's interactions with HP1 and CHD4 may direct distinct transcriptional programs at LADs, potentially influencing neural differentiation and developmental signaling through separate mechanisms.

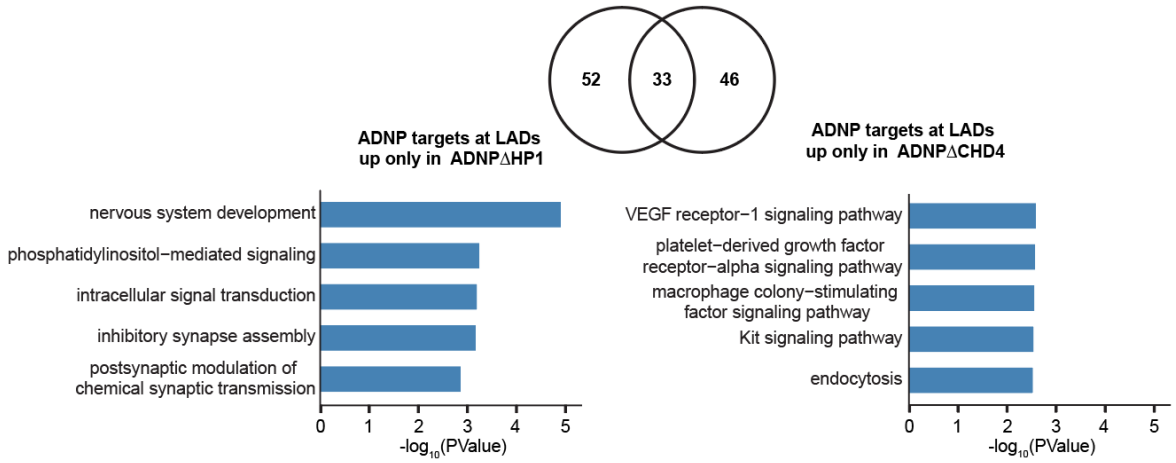


**Figure 18 HP1 and CHD4 interactions with ADNP repress different set of LADs--localized genes.**

Dot plot showing Biological process GO terms for upregulated ADNP target genes at LADs in ADNPΔHP1 and ADNPΔCHD4.

Finally, to determine whether ADNP loss or mutations have a general effect on chromatin association to the nuclear lamina, we performed ChIP sequencing for LaminB1. After ChIP, we defined LADs using EDD (Eivind Gard Lund, 2018). Overall, we did not observe a global

change in LADs distribution upon loss of ADNP or defects in ADNPΔHP1 or ADNPΔCHD4 interactions (Figure 19). Our results suggested that HP1-dependent positioning of ADNP at the nuclear lamina does not affect global genomic organization at the nuclei periphery.

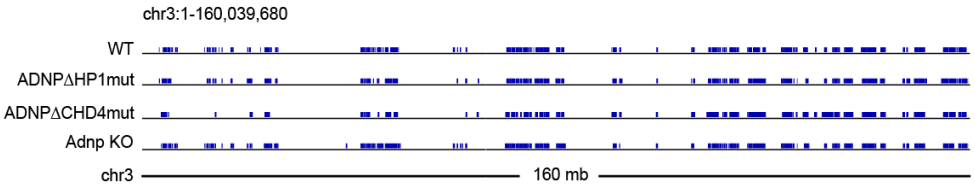


**Figure 19 ADNP interactions don't change global LADs distribution.**

Representative browser shot of LADs distribution on chromosome 3. The tracks indicate LADs in WT, ADNPΔHP1, ADNPΔCHD4 and ADNP KO.

### ADNP-HP1 interaction is required for pluripotency genes regulation

Given the central role of chromatin regulators in controlling lineage-specific transcriptional programs, we next turned our attention to the core pluripotency network in mESCs. Specifically, we focused on Nanog, Pou5f1 (Oct4), Sox2, and Klf4, the four key transcription factors responsible for maintaining stemness and self-renewal (Takahashi and Yamanaka, 2006). This allowed us to examine how chromatin dynamics mediated by ADNP and its interacting partners might intersect with the regulatory circuits that sustain pluripotency. Interestingly, ADNP localize on *Nanog* promoter and on *Pou5f1* distal gene body, but *Sox2* and *Klf4* seemed not to be ADNP targets (Figure 20A). ADNP binding on *Nanog* promoter showed a significant increase in ADNPΔHP1 cells and a slight decrease in ADNPΔCHD4, while ADNP binding on Pou5f1 did not seem to be affected in the mutants (Figure 20B). Notably, Nanog transcripts levels in ADNPΔHP1, but not ADNPΔCHD4, indicates clear transcriptional repression of this important pluripotency marker (Figure 20C). Pou5f1 showed a similar trend in ADNPΔHP1, while it appears to be upregulated in ADNPΔCHD4. The other two important markers, Sox2 and Klf4, did not present any difference in ADNPΔHP1 expression, while they were upregulated in ADNPΔCHD4 (Figure 20C).

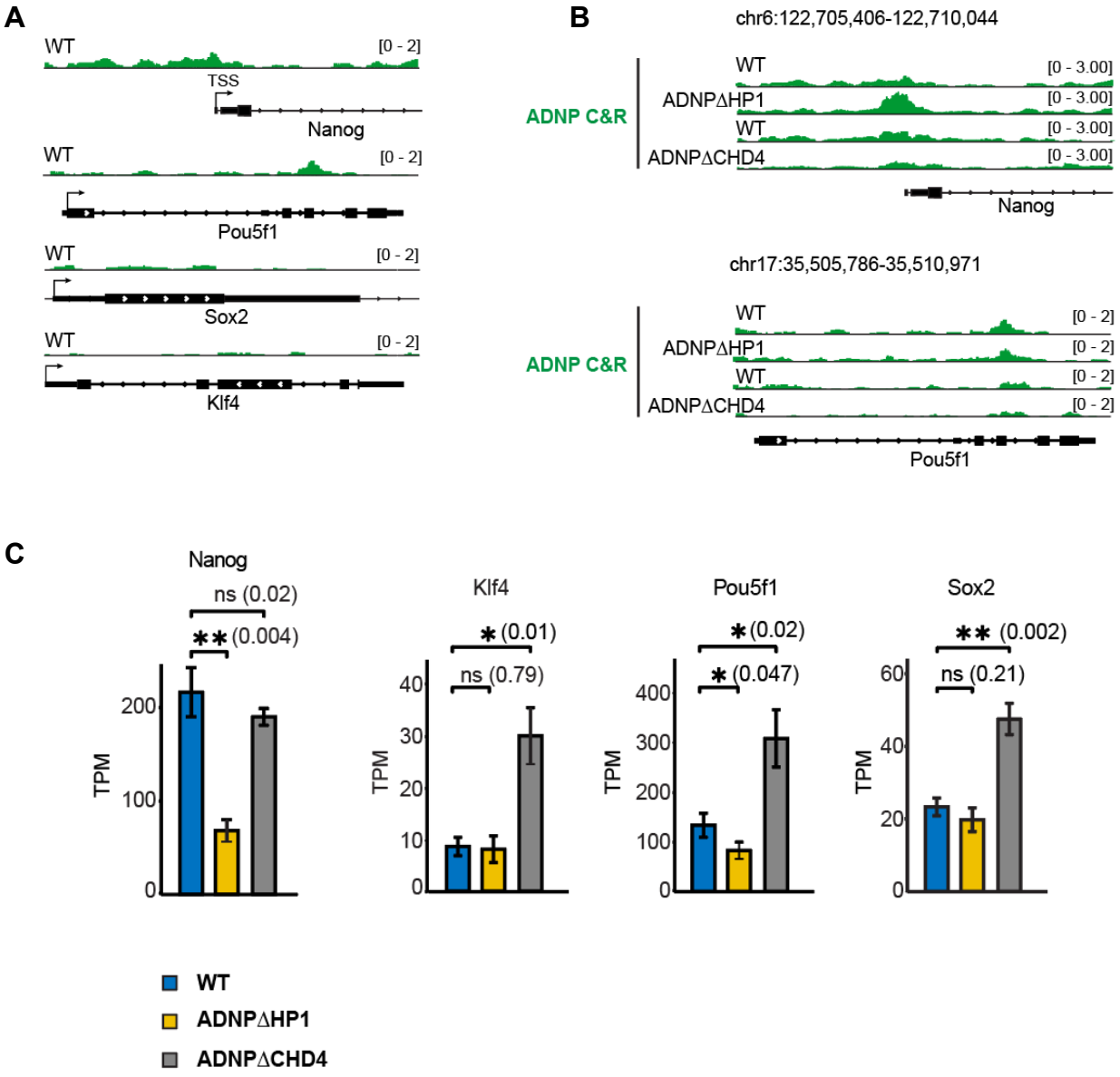


**Figure 20 ADNP-HP1 interaction regulates pluripotency markers expression.**

A) Browser view of ADNP CUT&RUN signal in WT mESCs on pluripotency markers. B) Browser view of ADNP CUT&RUN signal on Nanog promoter and Pou5f1 gene body. Tracks represent signal in WT, ADNPΔHP1 and ADNPΔCHD4 mESCs. C) Bar plots showing TPM expression from QuantSeq of pluripotency markers. Samples are WT (blue), ADNPΔHP1 (yellow) and ADNPΔCHD4 (grey) mESCs.

The gene regulatory network controlled by Nanog is highly complex. On one hand, Nanog represses genes responsible for differentiation; on the other, it promotes the transcription of factors involved in the maintenance of pluripotency. It was shown how depletion of Nanog

could destabilize the complex network that maintains pluripotency, leading to Pou5f1 repression (Mulas et al., 2024). One key Nanog target is Gbx2, a transcription factor involved in anterior neural patterning that is repressed by Nanog in mESCs (Heurtier et al., 2019). Similarly, Nanog inhibits the expression of Pou3f1 during the exit from pluripotency, delaying the onset of neural competence (Barral et al., 2019). This repression has downstream consequences: Pou3f1 is known to promote the activation of neural genes such as Pax6, which is essential for neuroectodermal specification, and Neurod1, a key driver of neuronal differentiation. For these reasons, we decided to examine the expression of all these genes by QuantSeq. Surprisingly, in the ADNPΔHP1 mutant, loss of Nanog-mediated repression leads to significant changes in the expression of several key factors. Gbx2, a direct Nanog target, is upregulated, as are Pax6, Pou3f1, and Neurod1. In contrast, ADNPΔCHD4 mutants do not display these changes (Figure 21).

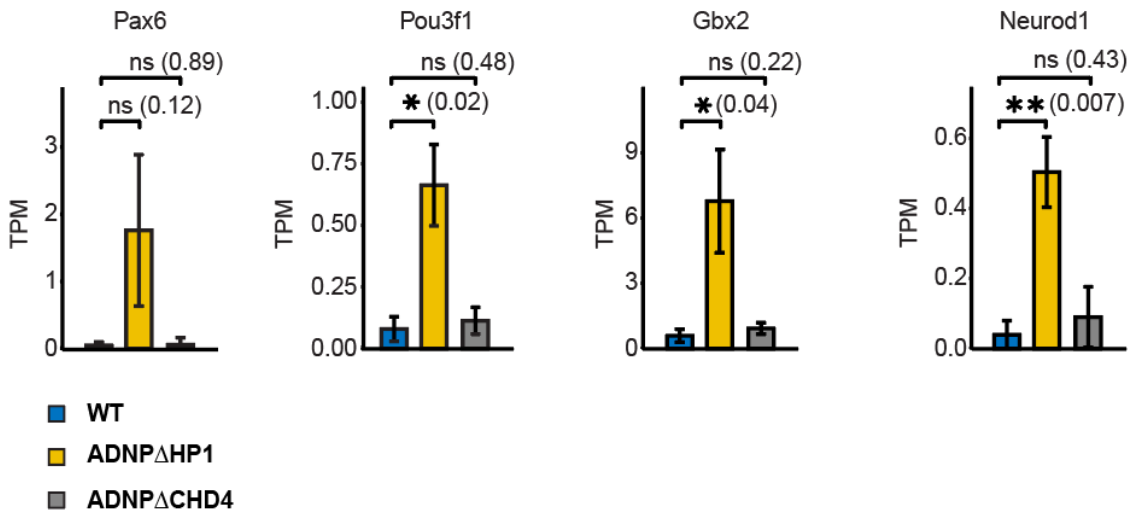


**Figure 21 Nanog repression correlates with target premature activation.**

Bar plots showing TPM expression from QuantSeq of Nanog downstream targets. Samples are WT (blue), ADNPΔHP1 (yellow) and ADNPΔCHD4 (grey) mESCs. At the bottom of each graph are showed p-values.

The premature Nanog repression , together with early activation and expression of neural markers, is frequently associated with a reduction in cellular pluripotency and precocious differentiation. This molecular dysregulation likely underlies the observed inability of ADNPΔHP1 ESCs to efficiently differentiate into neural progenitor cells (NPCs) in vitro, whereas wild-type and ADNPΔCHD4 cells maintain normal differentiation capacity. These results suggest that the ADNP–HP1 interaction is critical for maintaining the proper timing

of pluripotency exit and neural lineage early specification, while the ADNP–CHD4 interaction appears largely dispensable in this context.

## DISCUSSION

In this study, we investigated the specific roles of ADNP interactions with HP1 and CHD4 in chromatin regulation and neurodifferentiation by generating separation-of-function mutants. Our results reveal striking differences between ADNPΔHP1 and ADNPΔCHD4 cells, highlighting the distinct contribution of these interactions to genomic targeting, heterochromatin maintenance, retrotransposon silencing, and the regulation of pluripotency and neural genes.

ADNP heterozygous mutations cause ADNP syndrome, a neurodevelopmental disorder characterized by intellectual disability, developmental delays and autism spectrum disorders (Helsmoortel et al., 2014). ADNP deficiency leads to abnormal gene expression and disrupted lineage specification. In neuronal cells and patient-derived iPSCs carrying pathogenic ADNP mutations, this is associated with mislocalization of ADNP, reduced neuronal survival, and impaired neurite development (Bieluszewska et al., 2025; D'Incal et al., 2023; Gozes, 2020; Sun et al., 2020). The directed differentiation experiments demonstrated that while both mutants initially progress through the epiblast-like cell stage similarly to wild-type ESCs, only the HP1-binding-deficient ADNP mutant fails to efficiently form neural progenitor cells. ADNPΔHP1 cells recapitulate key aspects of the ADNP knockout phenotype, including impaired neurite extension and early cell death upon exiting the EpiLC stage, whereas ADNPΔCHD4 cells differentiate normally. The observation that only ADNPΔHP1 cells fail to differentiate highlights the critical role of the HP1 interaction motif, consistent with the fact that most pathogenic ADNP syndrome mutations introduce a premature stop codon upstream of this domain, likely disrupting HP1-mediated functions essential for neural lineage progression.

The differential chromatin localization of ADNP in the absence of HP1 or CHD4 provides mechanistic insight into how ADNP orchestrates distinct epigenetic programs during early neural development. Genome-wide profiling revealed that ADNPΔCHD4 cells exhibit moderate redistribution of ADNP binding, with increased occupancy at intergenic and intronic regions and reduced presence at promoters. In contrast, ADNPΔHP1 cells show highly selective changes, gaining ADNP at promoters while losing it from heterochromatic intergenic domains, including pericentromeres and Lamin-associated domains regions typically enriched for HP1 and associated with transcriptional repression and nuclear architecture maintenance (Lomberk et al., 2006; Ninova et al., 2019). These non-overlapping patterns suggest that HP1 and CHD4 mediate distinct recruitment mechanisms

for ADNP, with HP1 guiding ADNP to repressive chromatin and CHD4 facilitating its presence at active regulatory elements. The gain of ADNP at CTCF-enriched, SINE B2-rich loci in ADNPΔCHD4 cells is particularly intriguing, as it implies that ADNP may normally antagonize CTCF binding at these sites, potentially influencing chromatin loop formation and insulation (Kaaij et al., 2019). However, the dispensability of CHD4 for neural progenitor formation suggests that this architectural role is not essential for early lineage specification but may instead fine-tune chromatin topology or gene regulation at later stages. In contrast, the failure of ADNPΔHP1 cells to maintain heterochromatin integrity and silence retrotransposons aligns with prior evidence that HP1 is crucial for ADNP's role in safeguarding genome stability and promoting neuronal survival (Ostapcuk et al., 2018; Pinhasov et al., 2003; Vandeweyer et al., 2014). The overlap between ADNPΔHP1 phenotypes and those observed in ADNP knockout models further supports the notion that HP1-mediated recruitment is the dominant pathway for ADNP's neuroprotective functions. Given that most pathogenic mutations in ADNP syndrome truncate the protein upstream of the HP1-interacting domain, these findings provide a compelling molecular rationale for the observed neurodevelopmental deficits in patients. Together, these data reinforce a model in which ADNP operates through modular interactions to regulate chromatin accessibility, with HP1-dependent targeting to heterochromatin being indispensable for neural lineage fidelity, while CHD4-mediated recruitment contributes to architectural modulation

The selective loss of ADNP from pericentromeric heterochromatin in ADNPΔHP1 cells highlights a critical structural role for HP1-mediated recruitment in maintaining chromatin integrity during early neural differentiation. Despite HP1 localization remaining largely intact, the absence of ADNP at these regions leads to de-repression of major satellite repeats, clustering of pericentromeric domains, and increased nuclear area—hallmarks of heterochromatin decondensation. This suggests that ADNP itself, rather than HP1 alone, is required to preserve the compact architecture of pericentromeric chromatin, a domain enriched in H3K9me3 and known to be essential for genome stability (Ballmer et al., 2023; Mosch et al., 2011). These findings align with prior studies showing that HP1 recruits ADNP to H3K9me3-marked pericentromeric regions to silence repetitive elements and maintain nuclear compartmentalization. The structural disruption observed in ADNPΔHP1 cells underscores the importance of this interaction in organizing heterochromatin condensates, which are increasingly recognized as phase-separated domains critical for nuclear function (Novo et al., 2022). Disruption of the ADNP–HP1 interaction leads to loss of ADNP from pericentromeric regions while HP1 remains localized, coinciding with upregulation of major

satellite repeats. This suggests that although HP1 may serve as a structural scaffold, ADNP could be the key effector of functional silencing and architectural stabilization at these loci. However, further studies, such as direct HP1 knockout analyses, are needed to clarify HP1's independent contribution to satellite repression. In contrast, ADNPΔCHD4 cells exhibit more pronounced retrotransposon de-repression, yet retain the ability to differentiate into neural progenitors. This decoupling of transposable element silencing from differentiation capacity suggests that retrotransposon control, while important, is not the primary determinant of lineage progression. Instead, the structural integrity of pericentromeric heterochromatin, mediated by ADNP-HP1 interactions, appears to be more directly linked to successful neural commitment. This distinction is particularly relevant given that pericentromeric domains are known to influence nuclear organization and gene expression through long-range chromatin interactions (Stutzman et al., 2024). Taken together, these results reinforce the notion that ADNP's role in neurodevelopment is multifaceted, with HP1-dependent recruitment serving as a linchpin for heterochromatin maintenance and nuclear architecture, while CHD4-mediated functions contribute to transcriptional regulation and retrotransposon silencing. The differential impact of these pathways on differentiation outcomes provides a mechanistic framework for understanding how specific ADNP mutations, particularly those disrupting the HP1-interacting domain, lead to neurodevelopmental disorders such as ADNP syndrome.

The requirement of HP1 for ADNP localization to Lamin-associated domains (LADs) extends ADNP's structural and regulatory role beyond pericentromeric heterochromatin. LADs are large, gene-poor domains tethered to the nuclear lamina and typically associated with transcriptional repression and chromatin compaction. Despite the overall LAD distribution and nuclear lamina organization remaining intact in ADNPΔHP1 cells, the local loss of ADNP from these domains correlates with transcriptional de-repression of long neural-specific genes—suggesting that ADNP exerts a localized silencing function within LADs, rather than contributing to their global positioning (van Steensel and Belmont, 2017).This selective upregulation of long neural genes is particularly notable, as such genes often require additional regulatory oversight due to their complex transcriptional architecture and susceptibility to premature activation or splicing errors (Lopes et al., 2021; McCoy and Fire, 2020; Takeuchi et al., 2018; Zylka et al., 2015). The enrichment of ADNP at these loci implies a role in buffering transcriptional noise and ensuring precise timing of neural gene expression during the transition from pluripotency. HP1 likely facilitates this targeting by

anchoring ADNP to H3K9me3-marked heterochromatic regions within LADs, reinforcing a repressive chromatin environment until differentiation cues override it. Importantly, this mechanism appears distinct from ADNP's role in pericentromeric heterochromatin, which is more structural in nature. At LADs, ADNP–HP1 interactions serve a regulatory function, modulating gene expression without altering nuclear architecture. This duality reflects ADNP's versatility as both a chromatin organizer and a transcriptional regulator, depending on its genomic context. The implications for neurodevelopment are significant: disruption of ADNP–HP1 interactions, as seen in ADNPΔHP1 cells and likely in ADNP syndrome patients with truncating mutations upstream of the HP1-binding domain, may lead to premature or misregulated expression of neural genes, contributing to developmental delays and neuronal dysfunction. These findings reinforce the importance of local chromatin regulation at LADs in orchestrating the temporal dynamics of neural lineage commitment.

The regulatory role of ADNP–HP1 interactions extends into the control of pluripotency and early lineage commitment, acting as a molecular checkpoint that prevents premature neural induction. ADNP's direct binding to the *Nanog* promoter and *Pou5f1 (Oct4)* gene body, two core pluripotency regulators, positions it as a key modulator of the transition from self-renewal to differentiation (Gupta et al., 2023). In ADNPΔHP1 cells, increased ADNP occupancy at the *Nanog* promoter correlates with transcriptional repression, suggesting that HP1 may normally restrict ADNP's repressive activity at this locus, possibly by modulating its chromatin context or cofactor recruitment. This repression of Nanog is accompanied by early upregulation of downstream neural lineage genes such as *Gbx2, Pou3f1, Pax6,* and *Neurod1*, indicating a premature activation of neural differentiation programs. These genes are typically induced in a tightly regulated temporal sequence during neural commitment, and their early expression likely disrupts the balance between pluripotency maintenance and lineage progression (Soldati et al., 2012). This misregulation mirrors the phenotype of ADNPΔHP1 cells, which fail to maintain pluripotency and cannot efficiently generate neural progenitors, highlighting the functional importance of HP1-mediated ADNP recruitment in buffering the pluripotency-to-lineage transition. In contrast, ADNPΔCHD4 cells show minimal changes in these pathways, reinforcing the idea that CHD4-mediated recruitment of ADNP is dispensable for early lineage decisions. This divergence underscores the modularity of ADNP's interactions: while CHD4 may support architectural or repressive functions at specific loci, HP1 is essential for safeguarding developmental timing by anchoring ADNP to heterochromatic regions that regulate key transcriptional nodes. These findings align with broader models of chromatin-mediated developmental regulation, in

which heterochromatin-associated factors such as HP1 function not only as transcriptional repressors but also as temporal regulators, helping ensure that lineage-specific gene programs are activated with appropriate timing and developmental context. (Nicetto and Zaret, 2019). The disruption of this balance in ADNPΔHP1 cells provides a mechanistic explanation for the neurodevelopmental defects observed in ADNP syndrome, particularly in cases where truncating mutations eliminate the HP1-interacting domain.

Considering our findings, it becomes increasingly clear that ADNP's partnership with HP1 is not merely structural but functionally indispensable for maintaining heterochromatin integrity, particularly at pericentromeric regions, and for regulating long neural genes associated with lamina-associated domains (LADs). This interaction appears to act as a molecular gatekeeper, ensuring that the transition from pluripotency to neural commitment proceeds with appropriate timing and fidelity. The premature activation of neural genes observed in ADNPΔHP1 cells underscores the consequences of disrupting this checkpoint, leading to a cascade of transcriptional misregulation that compromises both pluripotency maintenance and lineage progression. By contrast, the ADNP–CHD4 axis, while contributing to chromatin targeting at specific loci such as CTCF-bound regions, seems dispensable for early neurodifferentiation. This distinction highlights a functional hierarchy within the ADNP interactome, where HP1 serves as the primary mediator of developmental timing, while CHD4 may play a more nuanced role in chromatin remodeling or transcriptional fine-tuning at later stages (Clémot-Dupont et al., 2025). These mechanistic insights carry broader implications for understanding ADNP syndrome, a neurodevelopmental disorder often linked to truncating mutations that disrupt the HP1-binding domain of ADNP. The resulting defects in heterochromatin organization, de-repression of repetitive elements, and dysregulation of neural-specific transcriptional programs likely contribute to the cognitive and developmental impairments observed in affected individuals (D'Incal et al., 2023). Altogether, our study positions the ADNP–HP1 interaction as a central node in the chromatin-based regulation of early neural fate decisions. It lays the groundwork for future research into how chromatin architecture and transcriptional networks are coordinated during development and how their disruption may be therapeutically targeted in neurodevelopmental disorders.

## FUTURE PERSPECTIVES

Given that most truncating mutations associated with ADNP syndrome occur before the HP1-binding domain, thereby preventing HP1 recruitment by approximately half of the total ADNP protein, our results point to a mechanistic link between impaired ADNP–HP1 interaction and the neurodevelopmental abnormalities characteristic of the syndrome. Future research should aim to directly test this hypothesis by developing both in vitro and in vivo models that faithfully recapitulate these truncations. Patient-derived induced pluripotent stem cells (iPSCs) differentiated into neural lineages could serve as a critical system to evaluate how loss of ADNP–HP1 interaction alters chromatin architecture, pericentromeric organization, and the timing of pluripotency exit. These models would allow assessment of whether heterochromatin decondensation and the misregulation of neural genes observed in ADNPΔHP1 cells also occur in patient contexts, thereby clarifying the contribution of HP1-dependent chromatin regulation to the disorder's etiology.

In parallel, animal models carrying engineered ADNP truncations lacking HP1-binding sites would enable investigation of how these molecular defects translate into developmental, behavioral, and neurological phenotypes. Such models could illuminate whether the loss of ADNP–HP1 coupling primarily affects early neural lineage commitment, synaptic maturation, or long-term neuronal maintenance. Importantly, these systems would also provide platforms to test therapeutic interventions aimed at restoring ADNP–HP1 function. Strategies might include expression of ADNP variants engineered to reconstitute HP1 binding, small molecules or peptides designed to stabilize HP1 recruitment, or epigenetic modulators that compensate for the loss of ADNP-mediated heterochromatin maintenance. Assessing their ability to rescue differentiation, neuronal morphology, or behavioral deficits would provide crucial translational insight.

To deepen mechanistic understanding, single-cell multiomic technologies integrating transcriptomic, chromatin accessibility, and methylation profiles across developmental stages could be employed to chart how disruption of ADNP–HP1 interaction perturbs cellular trajectories during neurogenesis. These analyses would help identify specific transcriptional regulators and chromatin modifiers whose dysregulation contributes to differentiation failure, potentially revealing new targets for intervention. By linking the molecular, cellular, and organismal consequences of ADNP–HP1 loss, such studies could uncover a coherent model of how defective heterochromatin organization and transcriptional misregulation drive the pathophysiology of ADNP syndrome. Ultimately, defining the functional hierarchy of

ADNP interactions and developing approaches to restore or compensate for lost HP1 coupling may provide a rational framework for therapeutic strategies aimed at mitigating the neurodevelopmental deficits associated with this disorder.

## MATERIALS AND METHODS

### Cell lines and cell culture

HEK293-T cells were cultured in DMEM (Corning MT10-013-CV) supplemented with 10% fetal bovine serum (Gibco) and 100 U/ml Pen-Strep. E14 mouse embryonic stem cells were cultured on 0.1% gelatin-coated plates in media containing DMEM (Corning MT10-013-CV), 15% fetal bovine serum (Gibco), 1x MEM non-essential amino acids, 1x GlutaMAX (Gibco 35050), 25 mM HEPES, 100 U/ml Pen-Strep, 55 μM 2-mercaptoethanol, 3 μM glycogen synthase kinase (GSK) inhibitor (Millipore 361559), 1 μM MEK1/2 inhibitor (Millipore 444966), and LIF (Sigma, ESGRO).

### Generation of ADNP-dHP1 and ADNP-dCHD4 mutants

To generate ADNP-dHP1 and ADNP-dCHD4 mutant cell lines with CRISPR/cas9, design of guide RNAs was carried out using the CRISPick tool (CRISPick) and inserted into PX459, a gift from Feng Zhang (Addgene plasmid: 62988) (Ran et al., 2013). To generate pCDNA3-ADNP donor plasmid, gBlock gene fragments were synthesized (IDT) and inserted into pCDNA3 using NEBuilder.

For the ADNPΔHP1 mutant, 1 μg guide RNA plasmid and 1 μg each of two donor plasmids were transfected into E14 mESCs. Candidate clones were selected by 1 μg/ml puromycin, screened by PCR on DNA isolated using QuickExtract (Epicentre QE09050) after BamHI digestion and further confirmed by Sanger sequencing.

For the ADNPΔCHD4 mutant, 1 μg guide RNA plasmid and 1.5 μg donor plasmid were transfected into E14 mESCs. Candidate clones were selected by 1 μg/ml puromycin, screened by PCR on DNA isolated using QuickExtract (Epicentre QE09050) and further confirmed by Western blot.

### Western blot and immunoprecipitation

mESCs were harvested and lysed in BC-500 buffer (50 mM Tris-HCl pH 7.6, 10% glycerol, 2 mM EDTA, 500 mM KCl, Roche cOmplete Protease Inhibitor). Whole cell extracts were quantified with Bio-Rad Protein Assay Dye Reagent (5000006) and equal amounts of protein were loaded for Western blot assay. Antibodies used for WB were anti-ADNP (in-house (Yan et al., 2022)), anti-CBX3 (Proteintech, 111650-2-AP, 1:1000), anti-CHD4 (Active Motif, clone

3F2/4, 39696, 1:1000) and anti-Actin (Sigma, A2066, 1:500). Briefly, proteins were separated on a NUPAGE 4-12% gradient SDS-PAGE gel and transferred to nitrocellulose membrane (400 mA constant, 90 min). After blocking with 5% (w/v) nonfat milk in TBST for 30 min at room temperature, the membrane was incubated overnight at 4 °C with the primary antibodies in TBST + 5% (w/v) BSA. Secondary antibody incubations were perfomed at room temperature for 1 hour using Anti-rabbit IgG (H+L) (DyLight(tm) 800 4x PEG Conjugate, CellSign, 50-195-941, 1:30000) or Anti-mouse IgG (H+L) (DyLight™ 800 4X PEG Conjugate, CellSign, 50-195-945, 1:15000).

For endogenous IP, total nuclear proteins were extracted from cells. Briefly, cells were washed with 1 ml PBS and resuspended in Buffer A (10 mM HEPES pH 7.9, 5 mM $MgCl_2$, and 0.25 M sucrose) containing 0.1% NP-40 and incubated on ice for 10 min. Cells were centrifuged at 6000 × *g* at 4 °C for 10 min. The supernatant (cytosol) was transferred to a new tube, and cell pellet was resuspended in BC-500. 1 mg of the extract was diluted to 1 µg/ml in BC-150 and incubated at 4 °C with ADNP antibody coupled to protein A agarose beads (Invitrogen, 15918-014 ). Bound proteins were washed twice with BC300-NP40(0.1%) buffer, once with BC150, and eluted with 100 µl of 0.1 M Glycine (pH 2.5), quenched with 10 µl of 1M Tris-HCl pH 8.8. 50 µl were used for Western blot.

**mESC differentiation into neural progenitor cells**

Differentiation of mESCs to NPCs was performed as previously described (Gouti et al., 2014). Briefly, 25,000 cells were plated into gelatin-coated wells of a 6-well plate and cultured overnight in mESC medium. To induce differentiation, mESC medium was replaced with N2B27 medium (50% Neurobasal medium, 50% DMEM/F-12 medium, 1 mM sodium pyruvate, 0.1 mM non-essential amino acids, 2 mM L-Glutamine, 0.5% Pen-Strep, 55 µM beta-mercaptoethanol, 40 µG/mL bovine serum albumin, 1x N-2 supplement, 1x B-27 supplement) containing 10 ng/mL human basic fibroblast growth factor (bFGF, Gemini Bio #300-112 P) at 0h, 24h and 48h. At 72h, 96 h and 120h after induction, media was replaced with N2B27 medium containing 500 nM smoothened agonist (SAG, Sigma #566661). Cells were imaged on day 6 after induction.

**CUT&RUN and RNA-Seq**

CUT&RUN was performed as previously described (Skene et al., 2018; Skene and Henikoff, 2017) using ADNP (in-house) or CTCF antibody (CellSignaling, 3418S). 2 million cells per replicate were washed three times and resuspended in 1 ml wash buffer. Cells were immobilized on Concanavalin A-coated beads by rotating at room temperature for 15 minutes and resuspended in 50 µL dig-wash buffer containing 2 mM EDTA. ADNP antibody or CTCF antibody was added to each tube and samples were rotated overnight at 4 °C. Rabbit IgG (Sigma I5006) was added to a non-specific control sample. Cells were washed once with dig-wash buffer and resuspended in 50 µL dig-wash buffer. Protein A-MNase was added to a final concentration of 700 ng/ml and samples were incubated at 4 °C for 1 h. Cells were resuspended in 100 µL dig-wash buffer and $CaCl_2$ was added to a final concentration of 2 mM for MNase activation. Samples were incubated in wet ice at 0 °C for 30 min. 100 µL 2x STOP buffer was added to stop reaction. Samples were incubated at 37 °C for 10 min to release digested DNA fragments, centrifuged at 4 °C at 16,000 × *g* for 5 min, and supernatants transferred to new tubes. 2 µL 10% SDS and 50 µg proteinase K were added, and samples were incubated at 70 °C for 10 min. DNA was purified using PCI and ethanol precipitation.

RNA samples were extracted using Trizol reagent (Invitrogen) and subjected to DNase digestion with Turbo DNase (Ambion AM2238). RNA samples were then rRNA-depleted using FastSelect -rRNA HMR (Qiagen) and converted to cDNA using Ultra II Directional RNA Library Prep Kit (NEB E7760).

**QuantSeq**

Libraries for differential gene expression studies were prepared using the Quant Seq 3' mRNA-Seq V2 Library Prep Kit FWD (Lexogen, Vienna, Austria) as per manufacturer's instructions starting with an input of 300ng of DNA-free total RNA and 15 cycles of final PCR amplification. Overall library size was determined using the 4200 Tapestation and the High-sensitivity DNA 5000 assay (Agilent, Santa Clara, CA) and libraries were quantitated using the Qubit 2.0 Fluorometer (Thermo Fisher, Waltham, MA). Libraries were pooled and Next Generation Sequencing with a single-end 100 bp run length was done on the Nextseq 2000 (Illumina, San Diego, CA). A minimum of 10M reads per sample was acquired for each sample.

**Lamin-B1 ChIP**

2 million cells per replicate were crosslinked with 1% formaldehyde for 10 min at room temperature and quenched with 125 mM glycine. Resulting pellets were flash frozen at -80 °C. ChIP was performed as previously described (Shah et al., 2023), using 2 µg of Lamin B1 antibody per replicate (ab16048, Abcam).

**Library preparation**

CUT&RUN DNA, LmnB1 ChIP DNA and RNA-Seq cDNA samples were end-repaired using End-Repair Mix (Enzymatics), A-tailed using Klenow exonuclease minus (Enzymatics), purified with MinElute columns (Qiagen), and ligated to Illumina adapters (NEB #E7600) with T4 DNA ligase (Enzymatics). Size selection for fragments >150 bp was performed with AMpure XP (Beckman Coulter). Libraries were PCR amplified with barcoded adapters for Illumina sequencing (NEB #E7600) using Q5 DNA polymerase (NEB #M0491) and purified with AMpure XP (0.8 X total volume). Lamin-B1 ChIP libraries were prepared using NEBNext Ultra II DNA Library Prep Kit (NEB #E7645) and PCR amplified using Q5. Sequencing was performed on a NextSeq 1000 instrument (Illumina) with 61 x 2 paired-end cycles.

**Sequencing analysis**

CUT&RUN reads were mapped to the mm10 mouse genome using Bowtie2 version 2.2.9 (Langmead and Salzberg, 2012) using default parameters and paired-end setting. Sorted BAM files were generated using SAMtools version 1.15.1 and peaks were called with MACS2 2.2.7.1 (Zhang et al., 2008), using the parameters “-f BAMPE -g mm --keep-dup all”. BigWig tracks were obtained using the bamCoverage function in deepTools version 3.5.1 (Ramírez et al., 2016) using the parameters “--binSize 5 --extendReads --blackListFileName”, which remove a subset of ENCODE blacklist regions (Amemiya et al., 2019). CUT&RUN BigWigs were normalized using the “--normalizeUsing CPM” function. Heatmaps and profile plots were generated using the computeMatrix and plotProfile functions in deepTools. Differential CUT&RUN analysis were performed in R version 4.2.1 using the DiffBind package, version 3.8.4. Differential binding was called using the edgeR method and an FDR cutoff of 0.05. Overlap between peaksets was defined through simple genomic overlap between regions.

RNA-Seq data were aligned using STAR version 2.7.9 (Dobin et al., 2013). RSEM version 1.3.3 (Li and Dewey, 2011) was used to obtain estimated counts. Differential analysis of RNA-Seq data was performed in R using the packages limma version 3.54.2 and edgeR version 3.40.2.

**Immunofluorescence and DNA-FISH**

For immunostaining, 100k cells per spot were spun down on slides (Fisherbrand™ Premium Superfrost™ Microscope Slides) using Cytospin. Cells were incubated for 8 minutes in cold CSKT buffer (100mM NaCl, 300mM sucrose, 10 mM Pipes pH 6.8, 3mM $MgCl_2 6H_2O$, 0,5% triton-X 100) and fixed with 4% PFA at room temperature for 10 minutes. For IF, samples were incubated with blocking buffer (0.1% Triton-100, 1% BSA in DPBS) for 30 min. Antibodies used for IF were anti-ADNP (in-house (Yan et al., 2022), 1:250), anti-CBX3 (Proteintech, 111650-2-AP, 1:400), anti-CHD4 (Cell Signaling, CHD4 (D4B7) Rabbit mAb #12011, 1:500) and anti-LaminB1 (Abcam, Anti-Lamin B1 antibody - Nuclear Envelope Marker ab16048, 1:400). ADNP, CBX3 and CHD4 primary antibodies were incubated for 2h at room temperature. LaminB1 primary antibody was incubated overnight at 4 °C. All washes were performed with blocking bufferfor 5 minutes at room temperature. For ADNP, CBX3 and CHD4 stained samples, it was used a secondary anti-Rabbit IgG antibody conjugated to the Alexa Fluor™ 555 (Invitrogen, Goat anti-Rabbit IgG (H+L) Highly Cross-Adsorbed Secondary Antibody A-21429, 1:500). For LaminB1 For DNA-FISH protocol, slides were pre-denatured at 60 °C with 2XSSC-5%-formamide and then incubated with 10 pmol of DNA probes for 2 minutes at 95 °C and O/N at 37°C. In both experiments, Vecta-Shield with DAPI was used to prepare slides for imaging.

**IF-FISH analysis**

After staining and taking 3D z-stack images of cells, the images were segmented using the "Pixel Classification Method" in the Ilastik software suite (Berg et al., 2019). The DNA FISH foci, nuclei, and the nuclear lamina were segmented, and the resulting probability maps were used as inputs for image analysis in CellProfiler 4.2.6 (Stirling et al., 2021). The "RelateObjects" module was used to calculate distance between foci and the nuclei perimeter, as demarcated by the lamin staining.

**Imaging mESCs in widefield and STORM**

Cells were imaged in HILO (highly inclined and laminated optical sheet) with the Oxford Nanoimager S microscope (ONI) (100x oil immersion objective, 1.45 NA, Hamamatsu Orca flash 4.0 CMOS camera, 200ms exposure time for conventional widefield and 15ms for STORM). This illumination angle allows for widefield imaging within a cell's nuclear volume. Prior to imaging, PBS storage buffer was exchanged for an oxygen-scavenging imaging buffer (1% GLOX (14mg glucose oxidase, 20 mg/mL catalase, 10mM Tris pH 8.0, 50mM NaCl),1% beta mercaptoethanol (βME, 14.3M pure stock solution), and 10% glucose in 50 mM Tris pH8, 10 mM NaCl buffer and deionized water). Healthy, Hoechst-stained nuclei with major satellite pericentromeric repeat regions well in-focus were identified and imaged sequentially in widefield (10 frames at 200ms exposure for both targets) with excitation by 640nm laser (AF647-labeled pericentromeric regions) followed by 405nm (nuclei) in the same field of view and z-position before STORM imaging of the same nucleus using the 640nm laser (30,000 fames at 15ms).

**STORM image processing and analysis**

*Processing*

Widefield: All widefield images were processed using an in-house FIJI macro (Schindelin et al., 2012). In brief, final widefield images of nuclei were projections of the average fluorescence intensity over 10 separate frames of the same field of view (200ms exposure).

STORM: All STORM images were drift-corrected after acquisition in Nanoimager software (NimOS v.1.16.4) and filtered for photon count (min: 500), and sigma in x and y (min:10, max: 250) before additional drift correction by AIM (Ma et al., 2024) if required. Final filtered and drift-corrected STORM images were then segmented using the DBSCAN algorithm for further analysis.

*Analysis*

Individual cluster density was calculated by dividing the number of localizations in a cluster by the total area of the cluster. The mean of all individual cluster densities within each cell was plotted for every genotype (WT n = 52 cells, HP1 n = 57 cells, CHD4 n = 56 cells, ADNPKO n = 42 cells ). These means were then compared using a Mann-Whitney U test.

**Table of Primers and DNA probes**

| Name | Sequence (5'-3') |
|---|---|
| **Cloning** | |
| ADNPΔHP1-donor-gBlock (left) | GACCCAAGCTTGGTACCGAGCTCGACAAACAGCCCTATCCCAC<br>CAGGCTGCATCTAGTCCACTGCAGGGGTGTTGGAAAAACCCAG<br>AATGGCCAGGACAAGACAAACGCACCTTCTCGGCTCAATCAGT<br>CTCCAGGCCTGGCCCCTGTGAAGCGCACGTATGAGCAGATGG<br>AGTTTCCACTGCTAAAAAAGCGGAAGCTGGAGGAGGATGCTGA<br>TTCCCCTAGCTGCTTTGAAGAGAAGCCAGAAGAGCCTGTTGTT<br>TTAGCTTTAGACCCCAAGGGTCATGAAGATGATTCTTATGAGGC<br>TAGGAAAAGCTTTCTCACAAAGTACTTCAACAAACAGCCTTATC<br>CCACCAGAAGAGAAATTGAGAAGTTAGCTGCCAGTCTATGGCTA<br>TGGAAGAGTGACATTGCCTCCCATTTCAGTAACAAGAGGAAGA<br>AGTGTGTCCGCGACT |
| ADNPΔHP1-donor-gBlock (right) | TCCCATTTCAGTAACAAGAGGAAGAAGTGTGTCCGCGACTGTG<br>AAAAGTACAAGGCAGGATCCTTGGCAGGTTTTAACATGAAAGAA<br>TTAAATAAAGTCAAACACGAGATGGATTTTGATGCTGAGTGGCT<br>GTTTGAAAATCACGATGAGAAAGACTCAAGAGTCAATGCTAGCA<br>AGACTGTTGACAAAAAGCATAACCTTGGGAAAGAAGATGATAGC<br>TTCTCAGATAGTTTTGAACATTTGGAAGAAGAATCCAATGGAAG<br>CGGGAGTCCTTTTGACCCTGTCTTTGAAGTTGAGCCTAAAATTC<br>CCAGTGATAATTTAACAAACAGCCCTATCCCACCAGGATCCATC<br>ACACTGGCGGCCGCTCG |
| ADNPΔCHD4-donor-gBlock (left) | AGACCCAAGCTTGGTACCGAGCTCGCCCACCACGAATCAGCTC<br>CCTTGCCAATGTTCCCCCCGGAACCTTTTGATCCACAGCGAAG<br>TCTAAATAAATACTGCTGTTAGAGTGAGGAAGAAACTTCTTTTGA<br>GATTTTCTTTTTTCTATGCAAATTGTTGGGTGATGAGAAAGAGAG<br>CTGTTTGCCTTCCGTGTTGGTCATCAAGGTCTGCGTGCATTGC<br>AACAGTGTCACCTGTGAGTTCCTGTGTCTGAAGCCGAGAAGAT<br>CCACAAAATGAGGCTTTTCCATAGTTGGTTTGTGTTTTTAACAAG<br>AAAATGGAGAGGCTTTTTGTTTGTTTTTGTTTTTGTTTTTTTGCC<br>TCTGACTTCTCTCTGAAACCAGCCAACAAGTACAACTAGCAATT<br>TTTAAAGATTTAGCAAGAACTTGCACTGAGTTTTCATTTACAGGA<br>GCACAAATAAAAATATTTGATTCAAAAATGCATCTGAGTTCTTTTA<br>ATTTTTCCTGCAGGAGAAACCTCTAAAAGTCATTGCCTTGCAGA<br>GTTTCTGGGAATGCCTGGGGGAGGAGCCTGGAACTTGTAACTG<br>CTTGCCTTGAGTAACCTTCTCACTCTGGTTTCTGTTCTGTTTTGT<br>TTCGTTTGTTTTTTAGATGCCCAAGTCCTATGAAGCTTTGGTACA<br>GCATGTCATTGAGGACC |
| ADNPΔCHD4-donor-gBlock (right) | GGTACAGCATGTCATTGAGGACCATGAACGGATAGGCTATCAG<br>GTCACTGCCATGATCGGACACACAAATGTTGTAGTTCCCCGAG<br>CCAAGCCCTTGATGCTGATAGCTCCCAAACCTCAAGACAAAAA |

| | |
|---|---|
| | GGGCATGGGACTACCACCACGAATCAGCTCCCTTGCTTCTGGA<br>AATGTCCGGTCGTTGCCATCACAGCAGATGGTAAACCGATTGTC<br>AATACCAAAGCCCAACTTAAATTCAACGGGAGTCAACATGATGT<br>CCAATGTTCACCTGCAGCAAAACAACTATGGAGTCAAATCTGTG<br>GGCCAGAGCTATGGTGTTGGCCAGTCAGTGAGGCTGGGACTA<br>GGTGGCAATGCTCCAGTTTCCATCCCTCAACAGTCTCAGTCCG<br>TGAAACAGTTACTTCCAAGTGGGAATGGGAGGTCTTTTGGGCT<br>AGGTGCTGAGCAGAGGCCCCCAGCAGCAGCCAGGTACTCCCT<br>GCAGACTGCCAACACCTCTCTACCCCCAGGCCAAGTGAAGTCT<br>CCCTCTGTGTCTCAGTCACAGGCATCTAGAGTATTAGGTCAGTC<br>CAGTTCTAAACCTCCACCAGCCGCCACAGGCCCTCCTCCAAGC<br>AACCACTGTGCCACTCAGAAGTGGAAAATCTGTACAATCTGTAA<br>CGAGCTTTTCCCTGAGAATGTCTATAGCGTTGTAACTGCTTGCC<br>TTGAGTGGCACTAGTAACGGCCGCCAGTGTGCT |
| ADNPΔHP1-gRNA-F | CACCGACAAACAGCCCTATCCCACC |
| ADNPΔHP1-gRNA-R | AAACGGTGGGATAGGGCTGTTTGTC |
| ADNPΔCHD4-gRNA1-F | CACCGTTGTAACTGCTTGCCTTGAG |
| ADNPΔCHD4-gRNA1-R | AAACCTCAAGGCAAGCAGTTACAAC |
| ADNPΔCHD4-gRNA2-F | CACCGACCACGAATCAGCTCCCTTG |
| ADNPΔCHD4-gRNA2-R | AAACCAAGGGAGCTGATTCGTGGTC |
| ADNPΔHP1-screening-F | GACAGCCTCAACCATCACTCT |
| ADNPΔHP1-screening-R | GGAAGACTCATCAGACCAGGT |
| ADNPΔCHD4-screening-F | CGTGCATTGCAACAGTGTCA |
| ADNPΔCHD4-screening-R | TGGAACGGCAATACGGACAA |
| **DNA-FISH probes** | |
| Major-Satellite | /5Alex647N/TCTTGCCATATTCCACGTCC |
| Fggy-Fw | TCGGTTCCCAATCGGACAAG |
| Fggy-R | ATTACCGCGACCGGTTGAAG |
| Tcf12-Fw | CGGTAGGTCGGCGTGTCATG |
| Tcf12-R | AGTCGGACGCAACCCAGTTG |

| | |
|---|---|
| Nrg1-Fw | GCCCGCGTTGCGACTTATAC |
| Nrg1-R | GCCTTGAACGCGCGCAGTAC |
| Zdhhc14 (control chr17)-Fw | AGCTGATCGTGGCGTTGATG |
| Zdhhc14 (control chr17)-R | AAGGTGCTTCGCGAAACCAC |
| Col2a1 (control chr15)-Fw | TCGGTTCGTACGCTTGCATG |
| Col2a1 (control chr15)-R | TGTTACGGGCTTGCGTGATC |
| Ccn5 (control chr2)-Fw | GACCAAGAGCGGACGTTGTG |
| Ccn5 (control chr2)-R | CGGGATACCGTTCGCCTATG |
| Secondary-targetADNP | /Atto565/ TAGCGCAGGAGGTCCACGACGTGCAAGGGTGT |
| Secondary-Controls | /Alexa647/ CACACGCTCTCCGTCTTGGCCGTGGTCGATCA |

# BIBLIOGRAPHY


Ahel, J., Pandey, A., Schwaiger, M., Mohn, F., Basters, A., Kempf, G., Andriollo, A., Kaaij, L., Hess, D., and Bühler, M. (2024). ChAHP2 and ChAHP control diverse retrotransposons by complementary activities. Genes Dev *38*, 554-568.

Amemiya, H.M., Kundaje, A., and Boyle, A.P. (2019). The ENCODE Blacklist: Identification of Problematic Regions of the Genome. Sci Rep *9*, 9354.

Atkinson, S., and Armstrong, L. (2008). Epigenetics in embryonic stem cells: regulation of pluripotency and differentiation. Cell Tissue Res *331*, 23-29.

Ballmer, D., Tardat, M., Ortiz, R., Graff-Meyer, A., Ozonov, E.A., Genoud, C., Peters, A.H., and Fanourgakis, G. (2023). HP1 proteins regulate nucleolar structure and function by secluding pericentromeric constitutive heterochromatin. Nucleic Acids Res *51*, 117-143.

Barral, A., Rollan, I., Sanchez-Iranzo, H., Jawaid, W., Badia-Careaga, C., Menchero, S., Gomez, M.J., Torroja, C., Sanchez-Cabo, F., Göttgens, B.*, et al.* (2019). Nanog regulates Pou3f1 expression at the exit from pluripotency during gastrulation. Biol Open *8*.

Berg, S., Kutra, D., Kroeger, T., Straehle, C.N., Kausler, B.X., Haubold, C., Schiegg, M., Ales, J., Beier, T., Rudy, M.*, et al.* (2019). ilastik: interactive machine learning for (bio)image analysis. Nat Methods *16*, 1226-1232.

Bertrand, N., Castro, D.S., and Guillemot, F. (2002). Proneural genes and the specification of neural cell types. Nat Rev Neurosci *3*, 517-530.

Bhat, A., Ghatage, T., Bhan, S., Lahane, G.P., Dhar, A., Kumar, R., Pandita, R.K., Bhat, K.M., Ramos, K.S., and Pandita, T.K. (2022). Role of Transposable Elements in Genome Stability: Implications for Health and Disease. Int J Mol Sci *23*.

Bieluszewska, A., Wulfridge, P., Fang, K.C., Hong, Y., Sawada, T., Erwin, J., Song, H., Ming, G.L., and Sarma, K. (2025). Transcriptomic Analysis Uncovers an Unfolded Protein Response in ADNP Syndrome. Mol Cell Biol *45*, 143-153.

Bonev, B., Mendelson Cohen, N., Szabo, Q., Fritsch, L., Papadopoulos, G.L., Lubling, Y., Xu, X., Lv, X., Hugnot, J.P., Tanay, A.*, et al.* (2017). Multiscale 3D Genome Rewiring during Mouse Neural Development. Cell *171*, 557-572.e524.

Briand, N., and Collas, P. (2020). Lamina-associated domains: peripheral matters and internal affairs. Genome Biol *21*, 85.

Brook, F.A., and Gardner, R.L. (1997). The origin and efficient derivation of embryonic stem cells in the mouse. Proc Natl Acad Sci U S A *94*, 5709-5712.

Buecker, C., Srinivasan, R., Wu, Z., Calo, E., Acampora, D., Faial, T., Simeone, A., Tan, M., Swigut, T., and Wysocka, J. (2014). Reorganization of enhancer patterns in transition from naive to primed pluripotency. Cell Stem Cell *14*, 838-853.

Bulut-Karslioglu, A., Perrera, V., Scaranaro, M., de la Rosa-Velazquez, I.A., van de Nobelen, S., Shukeir, N., Popow, J., Gerle, B., Opravil, S., Pagani, M.*, et al.* (2012). A transcription factor-based mechanism for mouse heterochromatin formation. Nat Struct Mol Biol *19*, 1023-1030.

Chen, T., and Dent, S.Y. (2014). Chromatin modifiers and remodellers: regulators of cellular differentiation. Nat Rev Genet *15*, 93-106.

Chuong, E.B., Elde, N.C., and Feschotte, C. (2017). Regulatory activities of transposable elements: from conflicts to benefits. Nat Rev Genet *18*, 71-86.

Clémot-Dupont, S., Lourenço Fernandes, J.A., Larrigan, S., Sun, X., Medisetti, S., Stanley, R., El Hankouri, Z., Joshi, S.V., Picketts, D.J., Shekhar, K.*, et al.* (2025). The chromatin remodeler ADNP regulates neurodevelopmental disorder risk genes and neocortical neurogenesis. Proc Natl Acad Sci U S A *122*, e2405981122.

D'Incal, C.P., Van Rossem, K.E., De Man, K., Konings, A., Van Dijck, A., Rizzuti, L., Vitriolo, A., Testa, G., Gozes, I., Vanden Berghe, W*., et al.* (2023). Chromatin remodeler Activity-Dependent Neuroprotective Protein (ADNP) contributes to syndromic autism. Clin Epigenetics *15*, 45.
De Luca, C., Gupta, A., and Bortvin, A. (2023). Retrotransposon LINE-1 bodies in the cytoplasm of piRNA-deficient mouse spermatocytes: Ribonucleoproteins overcoming the integrated stress response. PLoS Genet *19*, e1010797.
DeGroat, W., Inoue, F., Ashuach, T., Yosef, N., Ahituv, N., and Kreimer, A. (2024). Comprehensive network modeling approaches unravel dynamic enhancer-promoter interactions across neural differentiation. bioRxiv.
Diehl, A.G., Ouyang, N., and Boyle, A.P. (2020). Transposable elements contribute to cell and species-specific chromatin looping and gene regulation in mammalian genomes. Nat Commun *11*, 1796.
Dixon, J.R., Selvaraj, S., Yue, F., Kim, A., Li, Y., Shen, Y., Hu, M., Liu, J.S., and Ren, B. (2012). Topological domains in mammalian genomes identified by analysis of chromatin interactions. Nature *485*, 376-380.
Dobin, A., Davis, C.A., Schlesinger, F., Drenkow, J., Zaleski, C., Jha, S., Batut, P., Chaisson, M., and Gingeras, T.R. (2013). STAR: ultrafast universal RNA-seq aligner. Bioinformatics *29*, 15-21.
Dominguez, G., Wu, Y., and Zhou, J. (2024). Epigenetic Regulation and Neurodevelopmental Disorders: From MeCP2 to the TCF20/PHF14 Complex. Genes (Basel) *15*.
Du, A.Y., Chobirko, J.D., Zhuo, X., Feschotte, C., and Wang, T. (2024). Regulatory transposable elements in the encyclopedia of DNA elements. Nat Commun *15*, 7594.
Eivind Gard Lund, P.C. (2018). CollasLab/edd. (GitHub).
ENCODE (2012). An integrated encyclopedia of DNA elements in the human genome. Nature *489*, 57-74.
Farnung, L., Ochmann, M., and Cramer, P. (2020). Nucleosome-CHD4 chromatin remodeler structure maps human disease mutations. Elife *9*.
Fonseca-Carvalho, M., Veríssimo, G., Lopes, M., Ferreira, D., Louzada, S., and Chaves, R. (2024). Answering the Cell Stress Call: Satellite Non-Coding Transcription as a Response Mechanism. Biomolecules *14*.
Franke, V., Ganesh, S., Karlic, R., Malik, R., Pasulka, J., Horvat, F., Kuzman, M., Fulka, H., Cernohorska, M., Urbanova, J*., et al.* (2017). Long terminal repeats power evolution of genes and gene expression programs in mammalian oocytes and zygotes. Genome Res *27*, 1384-1394.
Fudenberg, G., Imakaev, M., Lu, C., Goloborodko, A., Abdennur, N., and Mirny, L.A. (2016). Formation of Chromosomal Domains by Loop Extrusion. Cell Rep *15*, 2038-2049.
Ghosh, R.P., and Meyer, B.J. (2021). Spatial Organization of Chromatin: Emergence of Chromatin Structure During Development. Annu Rev Cell Dev Biol *37*, 199-232.
Gouti, M., Tsakiridis, A., Wymeersch, F.J., Huang, Y., Kleinjung, J., Wilson, V., and Briscoe, J. (2014). In vitro generation of neuromesodermal progenitors reveals distinct roles for wnt signalling in the specification of spinal cord and paraxial mesoderm identity. PLoS Biol *12*, e1001937.
Gozes, I. (2020). The ADNP Syndrome and CP201 (NAP) Potential and Hope. Front Neurol *11*, 608444.
Gozlan, O., and Sprinzak, D. (2023). Notch signaling in development and homeostasis. Development *150*.
Grewal, S.I., and Moazed, D. (2003). Heterochromatin and epigenetic control of gene expression. Science *301*, 798-802.
Guenatri, M., Bailly, D., Maison, C., and Almouzni, G. (2004). Mouse centric and pericentric satellite repeats form distinct functional heterochromatin. J Cell Biol *166*, 493-505.

Gupta, S., Polit, L.D., Fitzgerald, M., Rowland, H.A., Murali, D., Buckley, N.J., and Subramaniam, S. (2023). Temporal transcriptional control of neural induction in human induced pluripotent stem cells. Front Mol Neurosci *16*, 1139287.
Helsmoortel, C., Vulto-van Silfhout, A.T., Coe, B.P., Vandeweyer, G., Rooms, L., van den Ende, J., Schuurs-Hoeijmakers, J.H.M., Marcelis, C.L., Willemsen, M.H., Vissers, L.E.L.M.*, et al.* (2014). A SWI/SNF-related autism syndrome caused by de novo mutations in ADNP. Nature Genetics *46*, 380-384.
Heurtier, V., Owens, N., Gonzalez, I., Mueller, F., Proux, C., Mornico, D., Clerc, P., Dubois, A., and Navarro, P. (2019). The molecular logic of Nanog-induced self-renewal in mouse embryonic stem cells. Nat Commun *10*, 1109.
Hoffmann, A., and Spengler, D. (2019). Chromatin Remodeling Complex NuRD in Neurodevelopment and Neurodevelopmental Disorders. Front Genet *10*, 682.
Horton, I., Kelly, C.J., Dziulko, A., Simpson, D.M., and Chuong, E.B. (2023). Mouse B2 SINE elements function as IFN-inducible enhancers. Elife *12*.
Hutnick, L.K., Huang, X., Loo, T.C., Ma, Z., and Fan, G. (2010). Repression of retrotransposal elements in mouse embryonic stem cells is primarily mediated by a DNA methylation-independent mechanism. J Biol Chem *285*, 21082-21091.
Ichiyanagi, T., Katoh, H., Mori, Y., Hirafuku, K., Boyboy, B.A., Kawase, M., and Ichiyanagi, K. (2021). B2 SINE Copies Serve as a Transposable Boundary of DNA Methylation and Histone Modifications in the Mouse. Mol Biol Evol *38*, 2380-2395.
Ilık İ, A., Yang, X., Zhang, Z.Z.Z., and Aktaş, T. (2025). Transcriptional and post-transcriptional regulation of transposable elements and their roles in development and disease. Nat Rev Mol Cell Biol *26*, 759-775.
Jensen, K.N., and Lorincz, M.C. (2018). HP1 proteins safeguard embryonic stem cells. Nature *557*, 640-641.
Jessell, T.M. (2000). Neuronal specification in the spinal cord: inductive signals and transcriptional codes. Nat Rev Genet *1*, 20-29.
Kaaij, L.J.T., Mohn, F., van der Weide, R.H., de Wit, E., and Bühler, M. (2019). The ChAHP Complex Counteracts Chromatin Looping at CTCF Sites that Emerged from SINE Expansions in Mouse. Cell *178*, 1437-1451.e1414.
Kalkan, T., Olova, N., Roode, M., Mulas, C., Lee, H.J., Nett, I., Marks, H., Walker, R., Stunnenberg, H.G., Lilley, K.S.*, et al.* (2017). Tracking the embryonic stem cell transition from ground state pluripotency. Development *144*, 1221-1234.
Kalkan, T., and Smith, A. (2014). Mapping the route from naive pluripotency to lineage specification. Philos Trans R Soc Lond B Biol Sci *369*.
Karimi, M.M., Goyal, P., Maksakova, I.A., Bilenky, M., Leung, D., Tang, J.X., Shinkai, Y., Mager, D.L., Jones, S., Hirst, M.*, et al.* (2011). DNA methylation and SETDB1/H3K9me3 regulate predominantly distinct sets of genes, retroelements, and chimeric transcripts in mESCs. Cell Stem Cell *8*, 676-687.
Kemp, J.R., and Longworth, M.S. (2015). Crossing the LINE Toward Genomic Instability: LINE-1 Retrotransposition in Cancer. Front Chem *3*, 68.
Khalil, A.M., and Driscoll, D.J. (2010). Epigenetic regulation of pericentromeric heterochromatin during mammalian meiosis. Cytogenet Genome Res *129*, 280-289.
Khandia, R., Saeed, M., Alharbi, A.M., Ashraf, G.M., Greig, N.H., and Kamal, M.A. (2022). Codon Usage Bias Correlates With Gene Length in Neurodegeneration Associated Genes. Front Neurosci *16*, 895607.
Kim, S., Lee, J., Koh, I.G., Ji, J., Kim, H.J., Kim, E., Park, J., Park, J.E., and An, J.Y. (2024). An integrative single-cell atlas for exploring the cellular and temporal specificity of genes related to neurological disorders during human brain development. Exp Mol Med *56*, 2271-2282.

Kishi, Y., and Gotoh, Y. (2018). Regulation of Chromatin Structure During Neural Development. Front Neurosci *12*, 874.
Kornberg, R.D., and Lorch, Y. (1999). Twenty-five years of the nucleosome, fundamental particle of the eukaryote chromosome. Cell *98*, 285-294.
Lachner, M., O'Carroll, D., Rea, S., Mechtler, K., and Jenuwein, T. (2001). Methylation of histone H3 lysine 9 creates a binding site for HP1 proteins. Nature *410*, 116-120.
Langmead, B., and Salzberg, S.L. (2012). Fast gapped-read alignment with Bowtie 2. Nat Methods *9*, 357-359.
Larson, A.G., Elnatan, D., Keenen, M.M., Trnka, M.J., Johnston, J.B., Burlingame, A.L., Agard, D.A., Redding, S., and Narlikar, G.J. (2017). Liquid droplet formation by HP1α suggests a role for phase separation in heterochromatin. Nature *547*, 236-240.
Lechner, M.S., Schultz, D.C., Negorev, D., Maul, G.G., and Rauscher, F.J., 3rd (2005). The mammalian heterochromatin protein 1 binds diverse nuclear proteins through a common motif that targets the chromoshadow domain. Biochem Biophys Res Commun *331*, 929-937.
Li, B., and Dewey, C.N. (2011). RSEM: accurate transcript quantification from RNA-Seq data with or without a reference genome. BMC Bioinformatics *12*, 323.
Lieberman-Aiden, E., van Berkum, N.L., Williams, L., Imakaev, M., Ragoczy, T., Telling, A., Amit, I., Lajoie, B.R., Sabo, P.J., Dorschner, M.O*., et al.* (2009). Comprehensive mapping of long-range interactions reveals folding principles of the human genome. Science *326*, 289-293.
Lomberk, G., Bensi, D., Fernandez-Zapico, M.E., and Urrutia, R. (2006). Evidence for the existence of an HP1-mediated subcode within the histone code. Nat Cell Biol *8*, 407-415.
Lopes, I., Altab, G., Raina, P., and de Magalhães, J.P. (2021). Gene Size Matters: An Analysis of Gene Length in the Human Genome. Front Genet *12*, 559998.
Lu, X. (2024). Regulation of endogenous retroviruses in murine embryonic stem cells and early embryos. J Mol Cell Biol *15*.
Ma, J., Wu, Y., Ma, L., Yang, X., Zhang, T., Song, G., Li, T., Gao, K., Shen, X., Lin, J*., et al.* (2024). A blueprint for tumor-infiltrating B cells across human cancers. Science *384*, eadj4857.
MacArthur, I.C., and Dawlaty, M.M. (2021). TET Enzymes and 5-Hydroxymethylcytosine in Neural Progenitor Cell Biology and Neurodevelopment. Front Cell Dev Biol *9*, 645335.
Maison, C., and Almouzni, G. (2004). HP1 and the dynamics of heterochromatin maintenance. Nat Rev Mol Cell Biol *5*, 296-304.
Mandel, S., Rechavi, G., and Gozes, I. (2007). Activity-dependent neuroprotective protein (ADNP) differentially interacts with chromatin to regulate genes essential for embryogenesis. Dev Biol *303*, 814-824.
Marks, H., Kalkan, T., Menafra, R., Denissov, S., Jones, K., Hofemeister, H., Nichols, J., Kranz, A., Stewart, A.F., Smith, A*., et al.* (2012). The transcriptional and epigenomic foundations of ground state pluripotency. Cell *149*, 590-604.
Martin, C.J., Oser, E.A., Nagarajan, P., Popova, L.V., Sunkel, B.D., Stanton, B.Z., and Parthun, M.R. (2025). Distinct classes of lamina-associated domains are defined by differential patterns of repressive histone methylation. Genome Res *35*, 1959-1974.
Martin, L., Vicario, C., Castells-García, Á., Lakadamyali, M., Neguembor, M.V., and Cosma, M.P. (2021). A protocol to quantify chromatin compaction with confocal and super-resolution microscopy in cultured cells. STAR Protoc *2*, 100865.
McCoy, M.J., and Fire, A.Z. (2020). Intron and gene size expansion during nervous system evolution. BMC Genomics *21*, 360.
Mosch, K., Franz, H., Soeroes, S., Singh, P.B., and Fischle, W. (2011). HP1 Recruits Activity-Dependent Neuroprotective Protein to H3K9me3 Marked Pericentromeric Heterochromatin for Silencing of Major Satellite Repeats. PLOS ONE *6*, e15894.

Mulas, C., Stammers, M., Salomaa, S.I., Heinzen, C., Suter, D.M., Smith, A., and Chalut, K.J. (2024). ERK signalling eliminates Nanog and maintains Oct4 to drive the formative pluripotency transition. Development *151*.
Muñoz-Sanjuán, I., and Brivanlou, A.H. (2002). Neural induction, the default model and embryonic stem cells. Nat Rev Neurosci *3*, 271-280.
Nicetto, D., and Zaret, K.S. (2019). Role of H3K9me3 heterochromatin in cell identity establishment and maintenance. Curr Opin Genet Dev *55*, 1-10.
Nichols, J., and Smith, A. (2009). Naive and primed pluripotent states. Cell Stem Cell *4*, 487-492.
Ninova, M., Fejes Tóth, K., and Aravin, A.A. (2019). The control of gene expression and cell identity by H3K9 trimethylation. Development *146*.
Notwell, J.H., Chung, T., Heavner, W., and Bejerano, G. (2015). A family of transposable elements co-opted into developmental enhancers in the mouse neocortex. Nat Commun *6*, 6644.
Novo, C.L., Wong, E.V., Hockings, C., Poudel, C., Sheekey, E., Wiese, M., Okkenhaug, H., Boulton, S.J., Basu, S., Walker, S.*, et al.* (2022). Satellite repeat transcripts modulate heterochromatin condensates and safeguard chromosome stability in mouse embryonic stem cells. Nat Commun *13*, 3525.
Ostapcuk, V., Mohn, F., Carl, S.H., Basters, A., Hess, D., Iesmantavicius, V., Lampersberger, L., Flemr, M., Pandey, A., Thomä, N.H.*, et al.* (2018). Activity-dependent neuroprotective protein recruits HP1 and CHD4 to control lineage-specifying genes. Nature *557*, 739-743.
Otterstrom, J., Castells-Garcia, A., Vicario, C., Gomez-Garcia, P.A., Cosma, M.P., and Lakadamyali, M. (2019). Super-resolution microscopy reveals how histone tail acetylation affects DNA compaction within nucleosomes in vivo. Nucleic Acids Res *47*, 8470-8484.
Park, J., Lee, K., Kim, K., and Yi, S.J. (2022). The role of histone modifications: from neurodevelopment to neurodiseases. Signal Transduct Target Ther *7*, 217.
Pașca, A.M., Park, J.Y., Shin, H.W., Qi, Q., Revah, O., Krasnoff, R., O'Hara, R., Willsey, A.J., Palmer, T.D., and Pașca, S.P. (2019). Human 3D cellular model of hypoxic brain injury of prematurity. Nat Med *25*, 784-791.
Percharde, M., Lin, C.J., Yin, Y., Guan, J., Peixoto, G.A., Bulut-Karslioglu, A., Biechele, S., Huang, B., Shen, X., and Ramalho-Santos, M. (2018). A LINE1-Nucleolin Partnership Regulates Early Development and ESC Identity. Cell *174*, 391-405.e319.
Peric-Hupkes, D., Meuleman, W., Pagie, L., Bruggeman, S.W., Solovei, I., Brugman, W., Gräf, S., Flicek, P., Kerkhoven, R.M., van Lohuizen, M.*, et al.* (2010). Molecular maps of the reorganization of genome-nuclear lamina interactions during differentiation. Mol Cell *38*, 603-613.
Pescosolido, M.F., Schwede, M., Johnson Harrison, A., Schmidt, M., Gamsiz, E.D., Chen, W.S., Donahue, J.P., Shur, N., Jerskey, B.A., Phornphutkul, C.*, et al.* (2014). Expansion of the clinical phenotype associated with mutations in activity-dependent neuroprotective protein. J Med Genet *51*, 587-589.
Pevny, L., and Placzek, M. (2005). SOX genes and neural progenitor identity. Curr Opin Neurobiol *15*, 7-13.
Pinhasov, A., Mandel, S., Torchinsky, A., Giladi, E., Pittel, Z., Goldsweig, A.M., Servoss, S.J., Brenneman, D.E., and Gozes, I. (2003). Activity-dependent neuroprotective protein: a novel gene essential for brain formation. Brain Res Dev Brain Res *144*, 83-90.
Polioudaki, H., Kourmouli, N., Drosou, V., Bakou, A., Theodoropoulos, P.A., Singh, P.B., Giannakouros, T., and Georgatos, S.D. (2001). Histones H3/H4 form a tight complex with the inner nuclear membrane protein LBR and heterochromatin protein 1. EMBO Rep *2*, 920-925.
Qian, X., Song, H., and Ming, G.L. (2019). Brain organoids: advances, applications and challenges. Development *146*.

Ramírez, F., Ryan, D.P., Grüning, B., Bhardwaj, V., Kilpert, F., Richter, A.S., Heyne, S., Dündar, F., and Manke, T. (2016). deepTools2: a next generation web server for deep-sequencing data analysis. Nucleic Acids Res *44*, W160-165.
Ran, F.A., Hsu, P.D., Wright, J., Agarwala, V., Scott, D.A., and Zhang, F. (2013). Genome engineering using the CRISPR-Cas9 system. Nat Protoc *8*, 2281-2308.
Rezazadeh, S., Ji, H., and Giulivi, C. (2025). Chromatin modifiers in neurodevelopment. Front Mol Neurosci *18*, 1551107.
Richardson, S.R., Doucet, A.J., Kopera, H.C., Moldovan, J.B., Garcia-Perez, J.L., and Moran, J.V. (2015). The Influence of LINE-1 and SINE Retrotransposons on Mammalian Genomes. Microbiol Spectr *3*, Mdna3-0061-2014.
Sanulli, S., Gross, J.D., and Narlikar, G.J. (2019). Biophysical Properties of HP1-Mediated Heterochromatin. Cold Spring Harb Symp Quant Biol *84*, 217-225.
Schindelin, J., Arganda-Carreras, I., Frise, E., Kaynig, V., Longair, M., Pietzsch, T., Preibisch, S., Rueden, C., Saalfeld, S., Schmid, B.*, et al.* (2012). Fiji: an open-source platform for biological-image analysis. Nat Methods *9*, 676-682.
Shah, P.P., Keough, K.C., Gjoni, K., Santini, G.T., Abdill, R.J., Wickramasinghe, N.M., Dundes, C.E., Karnay, A., Chen, A., Salomon, R.E.A.*, et al.* (2023). An atlas of lamina-associated chromatin across twelve human cell types reveals an intermediate chromatin subtype. Genome Biol *24*, 16.
Shi, Y., Kirwan, P., Smith, J., Robinson, H.P., and Livesey, F.J. (2012). Human cerebral cortex development from pluripotent stem cells to functional excitatory synapses. Nat Neurosci *15*, 477-486, s471.
Skene, P.J., Henikoff, J.G., and Henikoff, S. (2018). Targeted in situ genome-wide profiling with high efficiency for low cell numbers. Nat Protoc *13*, 1006-1019.
Skene, P.J., and Henikoff, S. (2017). An efficient targeted nuclease strategy for high-resolution mapping of DNA binding sites. Elife *6*.
Smeenk, G., Wiegant, W.W., Vrolijk, H., Solari, A.P., Pastink, A., and van Attikum, H. (2010). The NuRD chromatin-remodeling complex regulates signaling and repair of DNA damage. J Cell Biol *190*, 741-749.
Soldati, C., Bithell, A., Johnston, C., Wong, K.Y., Teng, S.W., Beglopoulos, V., Stanton, L.W., and Buckley, N.J. (2012). Repressor element 1 silencing transcription factor couples loss of pluripotency with neural induction and neural differentiation. Stem Cells *30*, 425-434.
Stevanovic, M., Drakulic, D., Lazic, A., Ninkovic, D.S., Schwirtlich, M., and Mojsin, M. (2021). SOX Transcription Factors as Important Regulators of Neuronal and Glial Differentiation During Nervous System Development and Adult Neurogenesis. Front Mol Neurosci *14*, 654031.
Stirling, D.R., Swain-Bowden, M.J., Lucas, A.M., Carpenter, A.E., Cimini, B.A., and Goodman, A. (2021). CellProfiler 4: improvements in speed, utility and usability. BMC Bioinformatics *22*, 433.
Stutzman, A.V., Hill, C.A., Armstrong, R.L., Gohil, R., Duronio, R.J., Dowen, J.M., and McKay, D.J. (2024). Heterochromatic 3D genome organization is directed by HP1a- and H3K9-dependent and independent mechanisms. Mol Cell *84*, 2017-2035.e2016.
Sun, X., Peng, X., Cao, Y., Zhou, Y., and Sun, Y. (2020). ADNP promotes neural differentiation by modulating Wnt/β-catenin signaling. Nat Commun *11*, 2984.
Takahashi, K., and Yamanaka, S. (2006). Induction of pluripotent stem cells from mouse embryonic and adult fibroblast cultures by defined factors. Cell *126*, 663-676.
Takeuchi, A., Iida, K., Tsubota, T., Hosokawa, M., Denawa, M., Brown, J.B., Ninomiya, K., Ito, M., Kimura, H., Abe, T.*, et al.* (2018). Loss of Sfpq Causes Long-Gene Transcriptopathy in the Brain. Cell Rep *23*, 1326-1341.

Tamaki, S., Suzuki, K., Abe, I., Endo, Y., Kakizawa, N., Watanabe, F., Saito, M., Tsujinaka, S., Miyakura, Y., Ohta, S.*, et al.* (2022). Overexpression of satellite RNAs in heterochromatin induces chromosomal instability and reflects drug sensitivity in mouse cancer cells. Sci Rep *12*, 10999.
van Steensel, B., and Belmont, A.S. (2017). Lamina-Associated Domains: Links with Chromosome Architecture, Heterochromatin, and Gene Repression. Cell *169*, 780-791.
Vandeweyer, G., Helsmoortel, C., Van Dijck, A., Vulto-van Silfhout, A.T., Coe, B.P., Bernier, R., Gerdts, J., Rooms, L., van den Ende, J., Bakshi, M.*, et al.* (2014). The transcriptional regulator ADNP links the BAF (SWI/SNF) complexes with autism. Am J Med Genet C Semin Med Genet *166c*, 315-326.
Velmeshev, D., Schirmer, L., Jung, D., Haeussler, M., Perez, Y., Mayer, S., Bhaduri, A., Goyal, N., Rowitch, D.H., and Kriegstein, A.R. (2019). Single-cell genomics identifies cell type-specific molecular changes in autism. Science *364*, 685-689.
Wang, J., Levasseur, D.N., and Orkin, S.H. (2008). Requirement of Nanog dimerization for stem cell self-renewal and pluripotency. Proc Natl Acad Sci U S A *105*, 6326-6331.
Wang, W., Gao, R., Yang, D., Ma, M., Zang, R., Wang, X., Chen, C., Kou, X., Zhao, Y., Chen, J.*, et al.* (2024). ADNP modulates SINE B2-derived CTCF-binding sites during blastocyst formation in mice. Genes Dev *38*, 168-188.
Wilson, S.I., and Edlund, T. (2001). Neural induction: toward a unifying mechanism. Nat Neurosci *4 Suppl*, 1161-1168.
Wu, H., D'Alessio, A.C., Ito, S., Wang, Z., Cui, K., Zhao, K., Sun, Y.E., and Zhang, Y. (2011). Genome-wide analysis of 5-hydroxymethylcytosine distribution reveals its dual function in transcriptional regulation in mouse embryonic stem cells. Genes Dev *25*, 679-684.
Wulfridge, P., Yan, Q., Rell, N., Doherty, J., Jacobson, S., Offley, S., Deliard, S., Feng, K., Phillips-Cremins, J.E., Gardini, A.*, et al.* (2023). G-quadruplexes associated with R-loops promote CTCF binding. Mol Cell *83*, 3064-3079.e3065.
Yan, Q., Wulfridge, P., Doherty, J., Fernandez-Luna, J.L., Real, P.J., Tang, H.Y., and Sarma, K. (2022). Proximity labeling identifies a repertoire of site-specific R-loop modulators. Nat Commun *13*, 53.
Ye, Q., Callebaut, I., Pezhman, A., Courvalin, J.C., and Worman, H.J. (1997). Domain-specific interactions of human HP1-type chromodomain proteins and inner nuclear membrane protein LBR. J Biol Chem *272*, 14983-14989.
Ye, Q., and Worman, H.J. (1996). Interaction between an integral protein of the nuclear envelope inner membrane and human chromodomain proteins homologous to Drosophila HP1. J Biol Chem *271*, 14653-14656.
Zhang, S., Bell, E., Zhi, H., Brown, S., Imran, S.A.M., Azuara, V., and Cui, W. (2019). OCT4 and PAX6 determine the dual function of SOX2 in human ESCs as a key pluripotent or neural factor. Stem Cell Res Ther *10*, 122.
Zhang, X., Celic, I., Mitchell, H., Stuckert, S., Vedula, L., and Han, J.S. (2024). Comprehensive profiling of L1 retrotransposons in mouse. Nucleic Acids Res *52*, 5166-5178.
Zhang, X., Huang, C.T., Chen, J., Pankratz, M.T., Xi, J., Li, J., Yang, Y., Lavaute, T.M., Li, X.J., Ayala, M.*, et al.* (2010). Pax6 is a human neuroectoderm cell fate determinant. Cell Stem Cell *7*, 90-100.
Zhang, Y., Liu, T., Meyer, C.A., Eeckhoute, J., Johnson, D.S., Bernstein, B.E., Nusbaum, C., Myers, R.M., Brown, M., Li, W.*, et al.* (2008). Model-based analysis of ChIP-Seq (MACS). Genome Biol *9*, R137.
Zylka, M.J., Simon, J.M., and Philpot, B.D. (2015). Gene length matters in neurons. Neuron *86*, 353-355.